Offshore Geothermal Energy Production

Study on the potential of reusing oil and gas reservoirs for geothermal electricity production in the Dutch offshore

Bachelor Thesis

Mathias Ruhe

Delft University of Technology

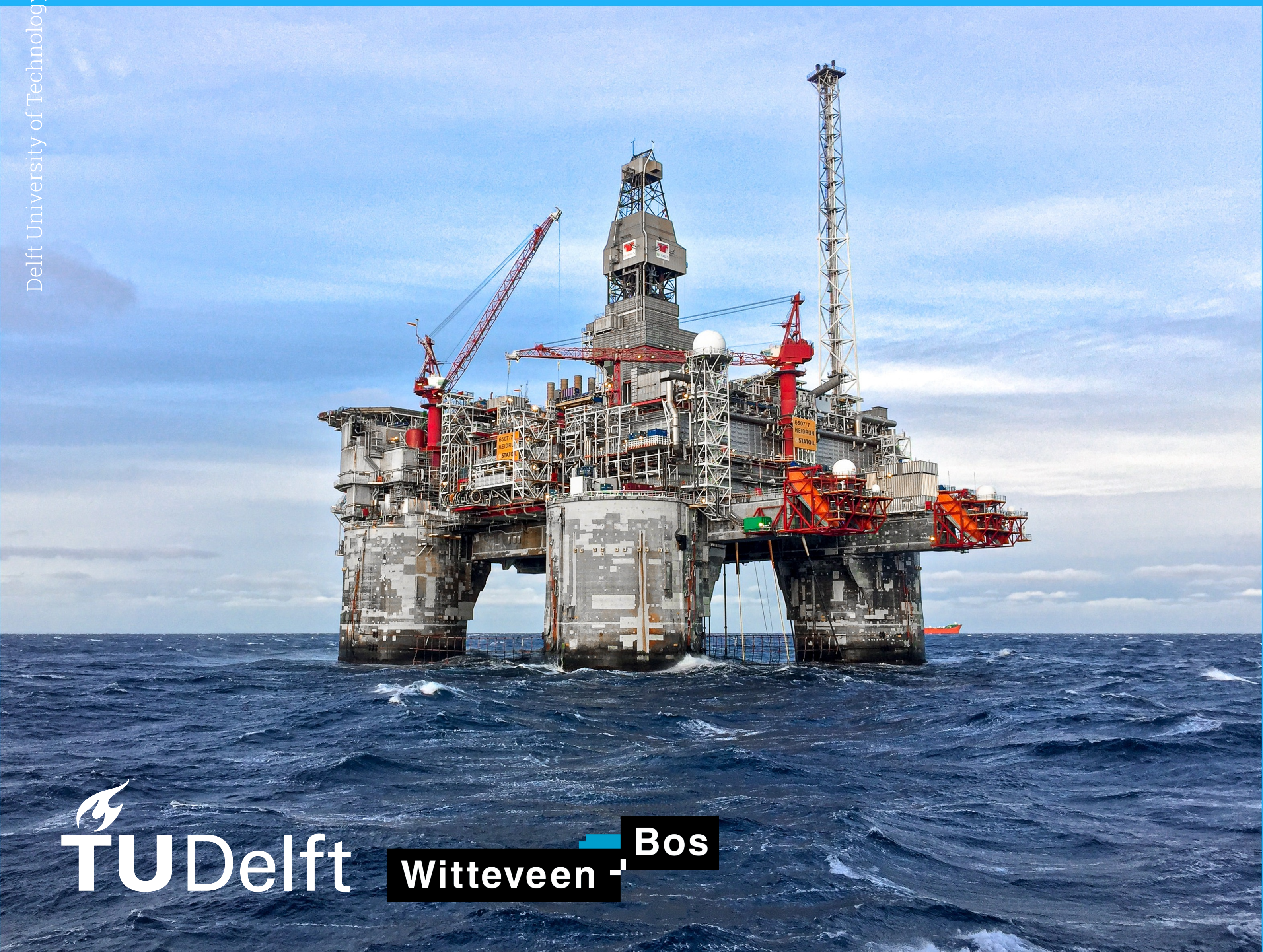

TUDelft

Witteveen + Bos

Offshore Geothermal Energy Production

Study on the potential of reusing oil and gas reservoirs for geothermal electricity production in the Dutch offshore

by

Mathias Ruhe

Student number:	5400880	
Project duration:	September 4, 2023 – 27 October, 2023	
Thesis committee:	Prof. dr. D. Bruhn,	TU Delft, supervisor
	Dr. A. Daniilidis,	TU Delft, supervisor
	Dr. A.M.H. Pluymakers,	TU Delft

Abstract

Reusing oil and gas reservoirs for geothermal energy production in the Dutch offshore could be an interesting energy resource for the energy transition. The Dutch offshore contains a large number of abandoned, and producing wells that are connected to hydrocarbon reservoirs. These reservoirs have undergone significant amounts of research, and large datasets are available on them. This reduces the need for expensive and extensive research. Additionally, developed reservoirs already have the necessary infrastructure used for production built around them, such as a platform, wells and technical equipment.

In this report a portfolio of reservoirs is constructed that have the highest probability of displaying an adequate geothermal potential for producing electricity. This is done by 1): assessing the reservoir wells on the temperature in the reservoir formation and 2): plotting the wells that show an adequate temperature over an interpolated permeability map. From this map the reservoirs with the highest formation temperatures and permeabilities are selected. The geothermal electricity production potential of the selected reservoirs is then evaluated by estimating their power output with DoubletCalc. To do so, the reservoirs are assumed to be laterally homogeneous on rock type, porosity, and permeability.

Of the 325 offshore reservoirs in the Netherlands, only 6 reservoirs met the required temperatures of over 120°C and an expected permeability of over 40mD. These cut-off values were introduced based on the fact that below these values the economic potential of a reservoir becomes riskful. Using the available data on NLOG an estimate of the power output could be made, which unfortunately resulted in low expected thermal power outputs (P50 < 1MW). This results from the low permeabilities in the aquifer layer, and lead to a low flow rate in the production well.
As the thermal energy needs to be converted to electricity, which only returns around 14% for a Binary conversion system, the electrical power estimates are not sufficient to make such projects economically viable. The reservoirs selected in this study are thus not suitable for development of geothermal electricity production. The output is too low and the costs to realize such a project would most likely be much larger than the potential of the project.

As these reservoirs were the best case scenario reservoirs from the reservoir selection process, the conclusion can be drawn that the hydrocarbon reservoirs in the dutch offshore are not good enough to reuse, as is. Further research should therefore be done on Enhanced Geothermal Systems (EGS). Here the permeability is enhanced through methods such as 'fracking', which could potentially increase the reservoir power output due to higher flow rates.

Acknowledgements

I want to thank Witteveen+Bos for their the opportunity support during my research on geothermal electricity in the Dutch offshore. Especially to my supervisors, Hans van 't Spijker and Liesbeth Jorissen, and Evan van der Voet for valuable insights into the research. Without their knowledge on the topic and availability during the project duration, I would not have been able to do as much as now.

I'm also grateful to my mentors at TU Delft, Alexandros Daniilidis and David Bruhn, for being an inspiration to me and guiding me where necessary.

And a special thanks to my thesis committee members, Alexandros, David, and Anne Pluymakers from TU Delft, for their valuable input.

I really enjoyed doing research on this topic and have leaned a lot during the past few months. This gives me new motivation into starting a master and doing research on topics regarding geothermal energy and reservoir engineering.

Mathias Ruhe
26-310-202

Contents

1
Introduction

Geothermal energy is considered a renewable energy source that, in contrast to other energy sources such as wind or solar energy, gives a constant reliable energy supply (Aydin and Merey, 2021). As the temperature in the reservoir remains constant over a long period of time, geothermal power plants are able to supply energy approximately 95% of the time (Salameh, 2014). On average the subsurface temperature rises with around 30 degrees Celsius per kilometer, which also allows for a predictable amount of heat that can be used as an energy source (Kabeyi, 2019). The energy generated from geothermal energy can be used in two different ways: direct heating projects or electricity generation projects (Aydin and Merey, 2021,Salameh, 2014). For direct heating purposes, geothermal power plants have to be build close to existing infrastructure to minimise heat loss during transportation. This limits the potential to built geothermal power plants in thinly populated areas. The other form of geothermal power production is converting the heat to electricity. This ensures that geothermal projects can be built in much more areas, further away from the energy consumers.

1.1. Motivation

The motivation to research the potential of repurposing hydrocarbon reservoirs for geothermal energy production stems from the fact that these reservoir have already been developed. There are a number of reasons why this strategy could be interesting (Aydin and Merey, 2021):

- The reservoirs and surrounding subsurface have already been extensively documented due to the exploration/production of gas and oil.
- The operational costs of geothermal energy are relatively low, the majority of the costs are formed by the drilling process which does not have to happen when the well is already there.
- besides the reservoir that is repurposed, this can also be done with the rest of the infrastructure such as th platform, production system, pumps, cables, etc. This leads to a very low carbon footprint.

The Dutch offshore counts a total of 325 out of 470 oil and gas reservoirs found in the Netherlands (“NLOG”, 2023), making it an area with a regional high density of reservoirs and good knowledge on the subsurface. For these reasons it should be considered to look into the possibilities of reusing oil and gas reservoirs for the purpose of geothermal energy in this area.

1.2. Approach

The goal of this study is as follows: through the usage of publicly available data, select a number of target reservoirs in the Dutch offshore that have the potential to be reused for geothermal projects. They are selected based on the following parameters: downhole temperature, reservoir properties, heat in place, technical potential, and proximity to offshore energy infrastructure. This portfolio of reservoirs should then be further evaluated on their technical potential.
The main questions that have to be answered are 1): which reservoirs in the Dutch offshore look good on paper for development of geothermal electricity production and 2): what is their technical potential

based on the data available? To do so, this report makes use of public available data on the Dutch offshore, such as temperature, porosity, and permeability data.
The report starts by investigating the relevant geological history to give a better insight into the Dutch offshore reservoirs. After this the methods to answering the previously mentioned research questions are described. A combination of literature, Python, QGIS, and DoubletCalc were used to generate results on the research questions.

2

Geology and Reservoir Quality of the Southern North Sea Basin

Understanding the regional geology gives insight on the development process of reservoirs. This will later in the study help with understanding the geothermal and reservoir properties at each well/reservoir. As this report only deems to find the layers most interesting for geothermal energy exploration, not the full history of the Southern North Sea (SNS) Basin will be discussed. It will be primarily limited to the historically important oil and gas layers, which are the early Triassic Buntsandstein sub group, and late Permian Rotliegend group with the Formation of Slochteren (Van Hulten, 2006). The majority of the oil and gas producing reservoirs are located in these formations due to a number of conditions that are just right, i.e. the presence of a permeable reservoir rock, a non-permeable reservoir seal, and a hydrocarbon source rock. This chapter will cover the deposition history, and structural event of the reservoir formations and discuss the effect this has had on the reservoir characteristics.

2.1. Geological history

The region of interest in this report is the Dutch part of the SNS Basin. The SNS Basin is part of the South Permian basin which refers to an area of ranging from the UK to Poland. Due to the high number of hydrocarbon reservoirs found here, including the famous the Groningen Gas field, a lot of geological research has been published that is relevant to this study.

2.1.1. Rotliegend and Triassic deposits

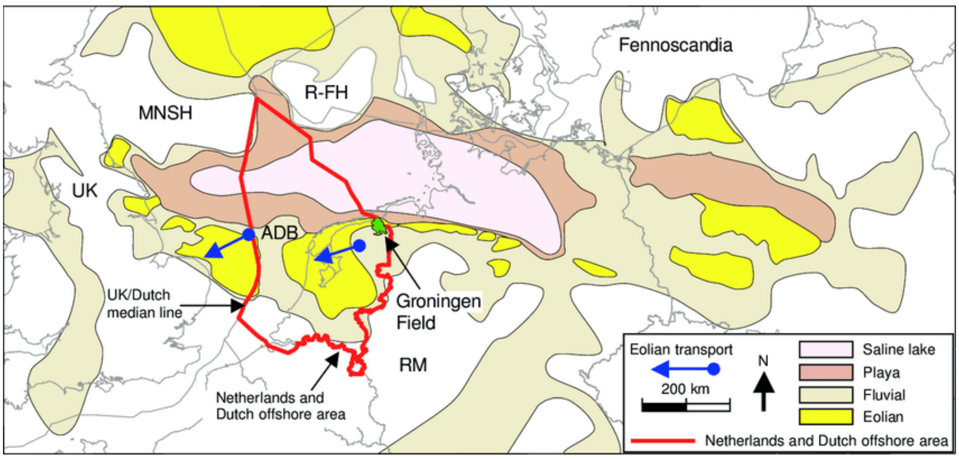

Figure 2.1: Overview of the different Rotliegend facies in the Dutch offshore (Mckie, 2011)

The sediments of the Rotliegend Group, to which the Slochteren Formation belongs to, were deposited in an arid environment. During the Carboniferous the region was located much more towards the equator with the Variscan Orogeny located southwards. The Variscan mountain range was the sediment source for the SNS Basin during the Permian ("Geode Atlas", 2023). Figure 2.1 gives an overview of the different facies during deposition of the Rotliegend: Along the southern margin of the SNS Basin, the Rotliegend consists of a combination of eolian and fluvial depositions, while the facies gradually turn into playa, and saline lake depositions. The Upper Rotliegend (formation of Slochteren) was deposited in an environment of dessert dunes and wadi's(van Gils et al., 2020). The Slochteren Formation itself consists of two main reservoir formations, the Upper- and Lower-Slochteren, and is separated by the shale layer of the Formation of Ameland (Verweij et al., 2011). This leads to the expectation that the porosity and permeability in the Rotliegend Group will be higher towards the south as eolian and fluvial depositions tend to consist of larger and better sorted grains. Playa and saline lake depositions, on the other hand, contain more clay, and evaporites who have a negative impact on porosity and permeability.

The formation on top of the Slochteren Formation is the Zechstein Formation. It was deposited in a shallow marine environment, leading to successions of shale, evaporite, and carbonate deposits ("Geode Atlas", 2023). The Zechstein Formation forms the top seal of the Upper-Rotliegend (Formation of Slochteren) reservoirs due to the impermeable evaporites, which ensure that the hydrocarbons remain trapped in the high quality reservoirs of the Upper-Rotliegend layer. The source rock of the hydrocarbons in the Upper-Rotliegend reservoirs are the underlying Carboniferous coal layers.

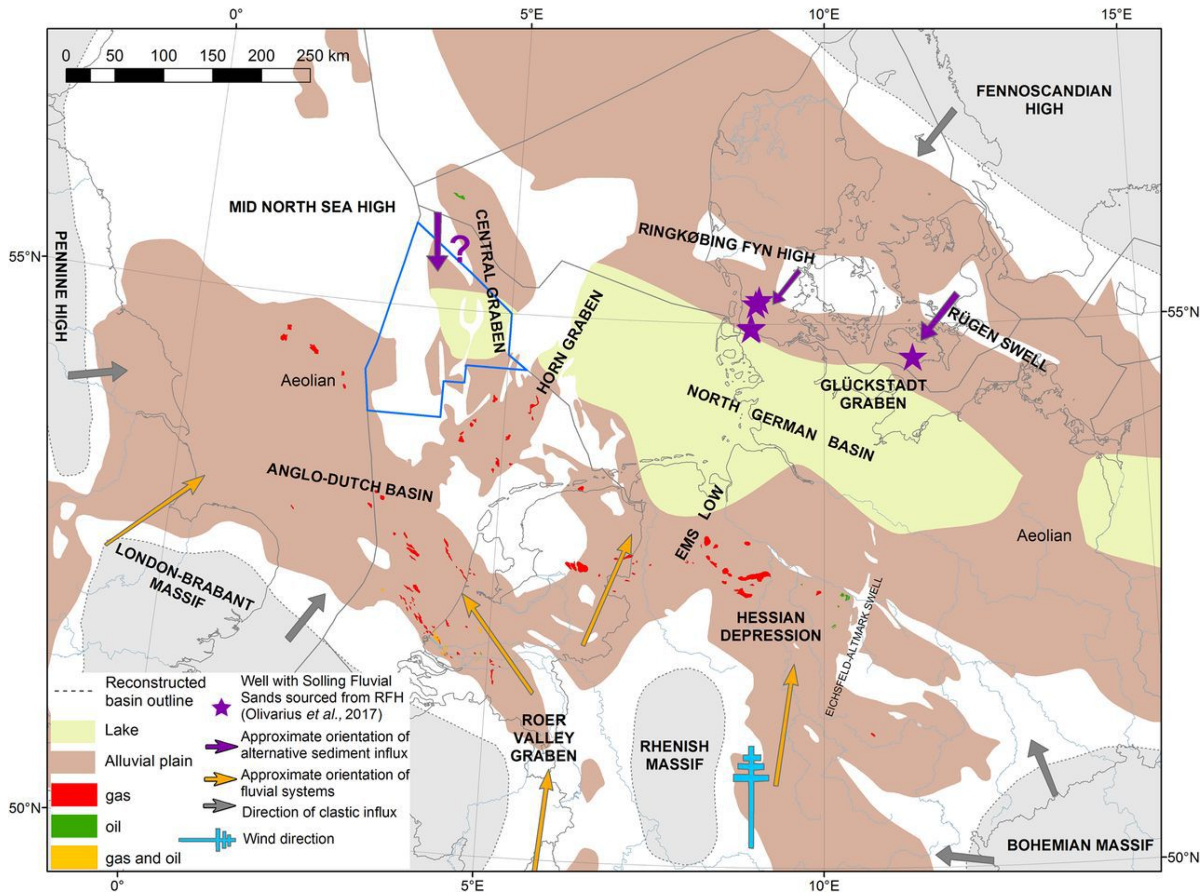

Figure 2.2: Overview of the different facies present during the Triassic (Kortekaas et al., 2018)

Figure 2.2 gives an overview of the Triassic facies found in the SNS Basin. Where the Rotliegend facies are a mix of eolian, fluvial, and saline lake sediments, the Triassic facies are mostly dominated by fluvial sediments. Occasionally alternating with eolian and playa deposits ("Geode Atlas", 2023). The main deposit environment during the Triassic in the Dutch offshore are alluvial plain deposits that consist of a mix of clay, silt, sand, and gravel (Editors of Encyclopaedia Britannica, 2020). The expectation therefore is that the porosity and permeability of the Buntsandstein layer will be lower than the Slochteren reservoir formation. This is due to the fluvial nature of the deposited layers, which can lead to deposition of more clay and silt in between the sandy layers (Editors of Encyclopaedia Britannica, 2020).

2.1.2. Geological structures SNS basin

Besides the geological deposition history it is important to shortly mention the different tectonic and structural events that shaped the Basin into its present form. An overview of the main structural elements of the SNS Basin can be found in figure 2.3. This starts with mentioning the Variscan orogeny that lasted from the late Devonian to the end of the Carboniferous. The subsequent eroding of the orogeny formed an important sediment source during the Permian (Barton, 1984). During the transition period from the Lower-Carboniferous to the Permian the South Permian Basin, not yet a basin during that period, experienced a phase of uplift associated with a mantle plume. This phase of uplift is the cause of the Base-Permian unconformity, found across the South Permian Basin. The end of the thermal unconformity, during the Permian also marks the beginning of the formation of the South Permian Basin due to subsidence related to crustal relaxation (Mahtab et al., 2019).

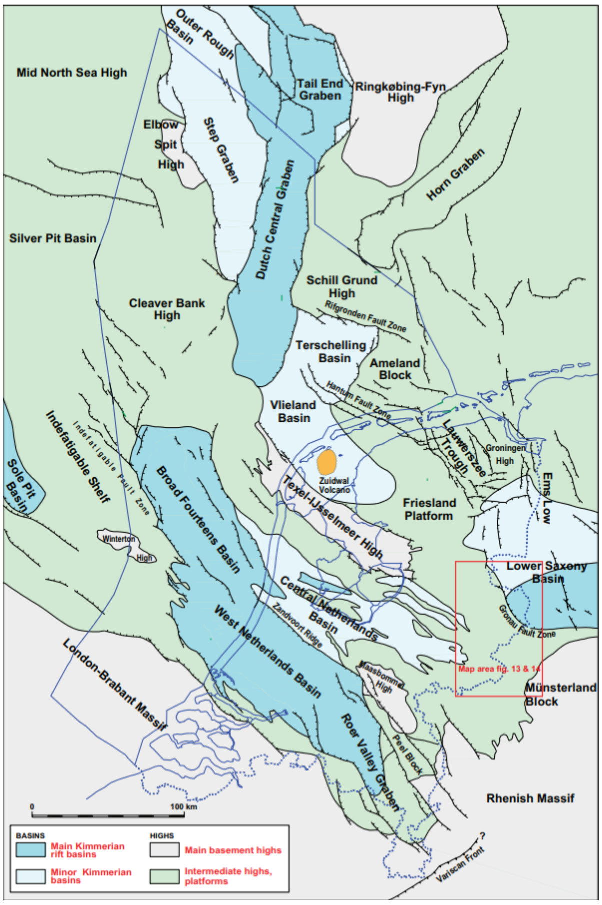

Figure 2.3: Structural elements in the Dutch on- and offshore (de Jager, 2007)

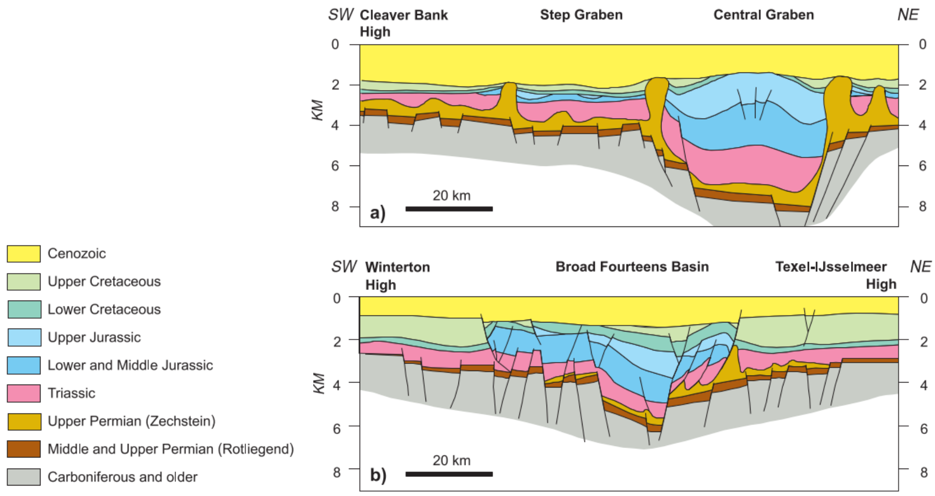

Figure 2.4: Cross section of the Dutch Central Graben and the Broad Fourteens Basin (de Jager, 2007)

The subsidence continued into the Triassic as Pangea started to break up. In figure 2.4 a cross section of both basins is given. The Triassic and Jurassic layers are much thicker in the middle of the basins, indicating that a lot of accommodation space was present during their deposition. These basins were created during the Middle-Jurassic, after a new thermal anomaly underneath the North Sea began to cool down. This created heavy rifting in the area and this major event lead to the creation of two major basins in the Dutch offshore: the Broad Fourteens Basin and the Central Dutch Graben. In both basins the main offshore reservoir formations (Triassic and Rotliegend) are buried at great depths. For the Rotliegend layer this is 4.5-6km in the Broad Fourteens Basin and 7-8km in the Dutch Central Graben.
During the Late-Cretaceous and Tertiary the region underwent inversion as a result of increasing stresses. The onset of this was the northwards movement of Africa which started the Pyrenees and Alpine Orogeny (de Jager, 2007). The major effect of this Inversion phase is that at present day cross section may not show the max depth at which reservoirs where buried, resulting in a higher compaction rate than expected. Therefore, leading to the problem that reservoir impairment might be a much greater issue than just by looking at burial depth. The amount of inversion is not everywhere similarly distributed evenly. Figure B.2 shows that some regions have experienced substantial amounts of inversion, and this higher risk of reservoir impairment. This is Especially the case for the Broad Fourteens Basin, and the Dutch Central Graben.

2.2. Reservoir quality

When talking about reservoir properties in general, porosity and permeability are key. Both properties can tell us how how much resources are stored, and what the behaviour of flow will be in the reservoir. In this case: geothermal heat stored in the pores and the flow rate of a well. The main reservoir layers in the Dutch offshore which are the Slochteren formation, part of the Rotliegend and Buntsandstein formation, part of the Triassic layers (“Geode Atlas”, 2023) are both sandstone layers. The porosity of the Rotliegend ranges from 5.5% to 26.9% with permeabilities of respectively 0.3mD t 2500mD (Van Hulten, 2006). Figure 2.5 gives an insight to what kind of porosity and permeability values are preferred for different types of geothermal systems. As the reservoir formations of the Rotliegend and Triassic are porous rocks and a hydrothermal is searched for, the minimum permeability is approximately 40mD for a porosity of 15%. For lower porosities and permeabilities a typical hydrothermal system is not suited but a Enhanced Geothermal System (EGS), whereby the permeability is increased artificially, could be an option (of US Department of energy, 2023).

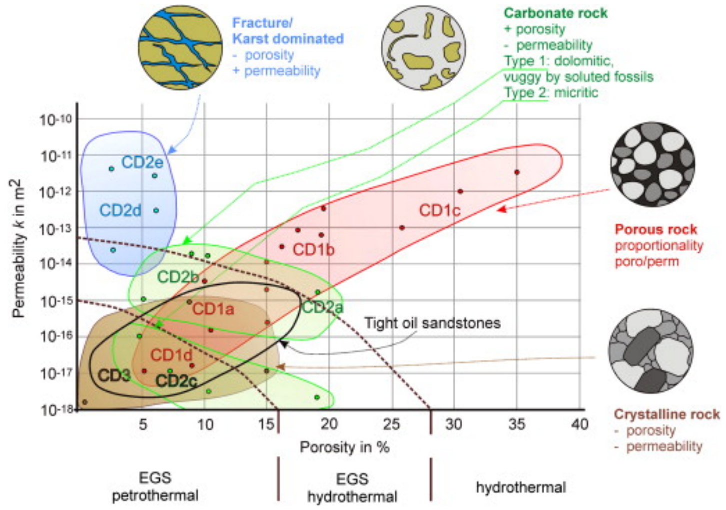

Figure 2.5: Porosity's and permeabilities associated with different rock formations and the possible geothermal systems that could be implemented Moeck, 2014

As the Rotliegend has been buried at great depths ($> 4km$) and experienced inversion, it is expected in some hydrocarbon reservoirs have low permeabilities resulting in tight oil and gas reservoirs. The porosities and permeabilities associated with such reservoirs are shown in figure B.1 of the appendix. For such reservoirs, EGS could be an interesting option, but as this is beyond the scope of this report it will merely be discussed in the recommendations.

3
Methodology

This chapter is split up into two sections: one for the methodology of the reservoir selection process and another one for the reservoir evaluation model.
In the first part the following will be discussed: models used for the reservoir selection process. The different steps of the section process itself, that consist of a reservoir characteristics evaluation using Python, and QGIS. Finally, the inaccuracies associated to the steps taken are mentioned.
The second part discusses the method on estimating the Recoverable heat, and power output of the selected reservoirs. For this Python and Doubletcalc were used. For the reservoir models a lot of assumptions had to be made as there is no real development plan each reservoir. These assumptions, and their inaccuracies will be discussed in the section.

3.1. Reservoir selection process and decision parameters

For a proper assessment of depleted oil and gas reservoirs on their reusability for extraction of geothermal energy, the parameters on how is decided which fields can be marked as 'interesting for geothermal exploration' need to be defined first. This will be done by evaluating the available reservoir temperature data and petrophysical properties. The data that was used for this study is all publicly available through public databases. The following is an overview on what data is used from which database:

- SNS pressure and temperature database: database from TNO containing pressure, and temperature data on a large number of wells in the Netherlands (both onshore and offshore). The formation temperatures and geothermal gradients are calculated using this database.
- NLOG (Dutch Oil and Gas Portal): main database used for the porosities, permeabilities, thicknesses and other reservoir characteristics. This database is also used for most of the data that makes up the reservoir selection model in QGIS

There are a total of 831 unique wells, of which data is stored in the SNS pressure and temperature database, in the Dutch offshore. These wells have to be evaluated based on their temperature and linked to one of the 325 offshore reservoirs that they belong to. Some wells were drilled as exploration wells and therefore do not have a reservoir connected to them, thus can be disregarded immediately.
The process of selecting the most suitable wells and reservoirs was done through the use of Python, QGIS, Excel, and available literature. Python was used for the temperature evaluation as this made it fairly easy to process large amounts (>12,000 datapoints) of offshore temperature and pressure at different depths and from different wells.

3.1.1. Flowcharts

As the reservoir selection was a process with a lot of parameters, flowcharts were made to give a clear overview of this process. From the data in the SNS database it could already be observed that the temperatures in the Triassic layers were barely reaching 100° C. Therefore it was decided to disregard these reservoirs in the methods and only focus on the reservoirs of the Rotliegend. The process of selecting the wells with sufficient temperature in the Rotliegend are shown in figure 3.1. For this the maximum Rotliegend temperature of each well was used. Geothermal systems are classified into two different systems: low-temperature systems (<150° C), and high-temperature systems (>150° C) (Sharmin et al., 2023). For the generation of electricity in general temperatures of over 100° C are requested (Guzović et al., 2010), although with practical considerations such as system efficiency: the higher the temperature, the better. As this study focuses on the potential of generating electricity from wells a cut-off temperature of 120°C is introduced, as can be seen in the temperature selection flowchart (figure 3.1). Electricity production is possible from 100°C but for practical considerations (temperature loss during the pumping phase) the temperature should be significantly higher than this.

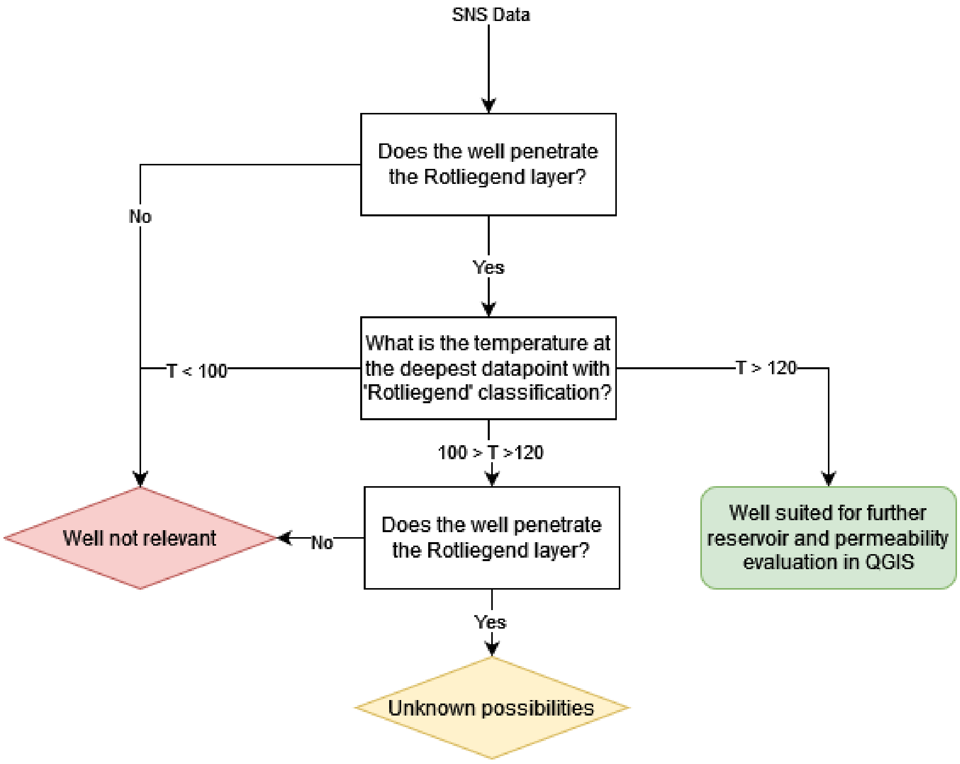

Figure 3.1: Flowchart used for evaluation of the reservoir temperatures using Python

The wells that showed a sufficient temperature in the Rotliegend were then used for further selection in QGIS. This second phase was to further investigate if certain wells were connected to reservoirs, what the approximate permeability range in the reservoirs were and what the surrounding area in the Rotliegend formation looked like (i.e. faults, top Rotliegend and thickness of the Rotliegend layer). This was all done visually: by looking if the well names matched with the reservoir names and if the reservoirs had regions of permeability higher than 40mD.

This is the minimum permeability at which a reservoir can be considered as 'interesting' in the Rotliegend play. According to a study by EBN on the potential of geothermal energy in the Netherlands van Gils et al., 2020, the lowest permeability before a reservoir is considered to be risky is 60mD. For this project a threshold value of 40mD for permeability is used due to due to the following reason: The study referred to marks reservoirs with low permeability as risk full but does not use a cut-off value. As the dutch offshore Rotliegend play has seen some regional inversion, the values are already expected to be lower than normally found at depths of 3-4km. Reducing the cut-off permeability therefore ensures that not all reservoirs are immediately disregarded.

The data used for the QGIS model was all obtained through public available data on the NLOG website such as permeability, thickness, and reservoir location maps. The QGIS model is build-up of multiple layers of data. Not all of them are meant for the reservoir selection process but also for extrapolating data from the selected reservoir for the reservoir evaluation process. In total there are 7 different layers of data used in the model:

- kriging interpolated permeability of the Lower-Slochteren (“Thermogis”, 2023)
- kriging interpolated permeability of the Upper-Slochteren (“Thermogis”, 2023)
- interpolated thickness of the Rotliegend (“NLOG”, 2023)
- interpolated top depth of the Rotliegend (“NLOG”, 2023)
- layer with the shape and names of all the offshore reservoirs (“NLOG”, 2023)
- All the major Zechstein(ZE) faults in the Dutch offshore (“NLOG”, 2023)
- All the minor Rotliegend(RO) faults in the NPC-2F area. (“NLOG”, 2023)

The fault shape files are imported to assist in estimating the geometry of the reservoirs after the reservoir selection process has taken place. Altough these faults are from the Zechstein Group, Looking at the contour lines and reservoir top maps suggest that most of them also run into the Rotliegend.
Figures of the model can be found in the appendix: B.4, B.6. These are the exact maps that were used for the reservoir selection process, of which the workflow is given by figure 4.2. By using the models and the locations of the wells from the previous step, the final selection could be made.

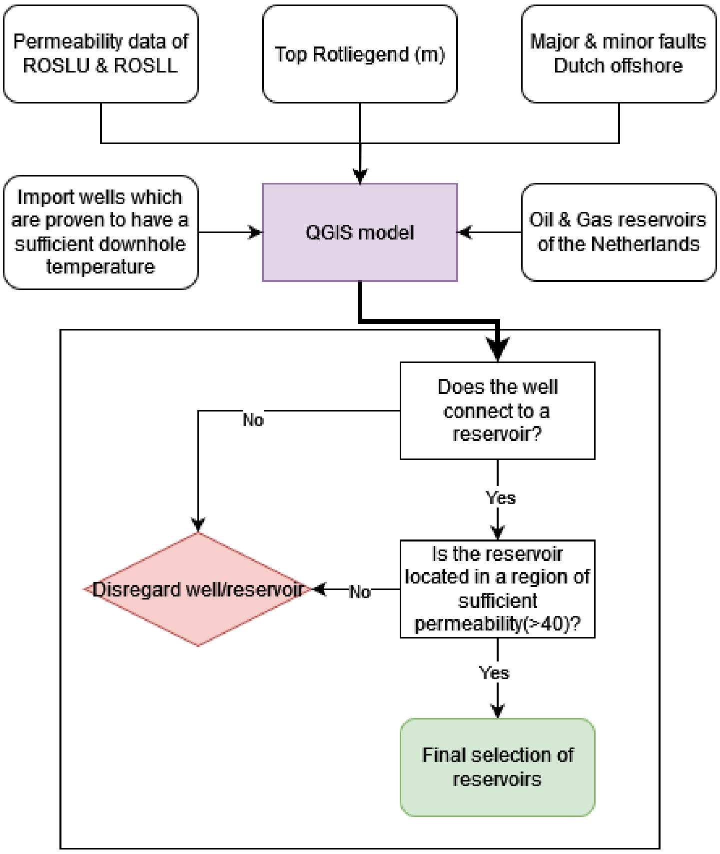

Figure 3.2: Flowchart used for reservoir selection process in QGIS

3.1.2. Surrounding infrastructure

The Dutch offshore is an area with relative high density of underwater infrastructure. Consisting of oil and gas transportation pipes, electricity cables, and data-transfer cables. The offshore geothermal platforms would be connected to a network of electricity cables to export their power to the shore. As these cables require tremendous investments, it is best to make use of the infrastructure in place instead of building it. Therefore the reservoirs deemed most interesting from the geothermal properties are also assessed on their proximity to existing or planned electricity infrastructure in the Dutch offshore. This is done by using the wind farm data files provided by Witteveen+Bos, and comparing the locations of the selected reservoirs to the locations of the offshore wind farms.
This report does investigate to what extend it is possible to connect geothermal electricity cables to wind farm electricity cables, and what agreements have to be closed in order to achieve this. This is beyond the scope of the research.

3.2. Heat in plave and recoverable heat

The reservoirs selected on with the methods described above are then evaluated on their resources and technical potential. The following section described the estimation of resources available in the reservoirs.

The total heat in place (HIP) of a geothermal reservoir q_r can be calculated by taking into account the reservoir volume and heat capacity & density properties of the reservoir rock and pore fluid (Garg and Combs, 2015). This equation given an estimate on the amount of heat stored in the tota reservoir, consisting of *pore fluid* and *reservoir rock*:

$$q_r = V(\phi S_l \rho_l c_l + \phi S_g \rho_g c_g + (1-\phi)\rho_r c_r)(T_R - T_r)$$

Where:

- V = volume(m^3)
- T_R, T_r = The average reservoir temperature and reference temperature($°C$)
- S_l, S_g = the liquid and steam saturation in the pores (-)
- ρ_l, ρ_g, ρ_r = density of the liquid, steam and reservoir rock (kg/m^3)
- c_l, c_g, c_r = heat capacity of liquid, steam and rock (J/kgK)
- ϕ = the average porosity(%)

The reference temperature T_r will be set to the minimum production temperature, i.e. below this temperature the production will stop. For simplification the reference temperature will be set to 100$°C$. This gives an overview of the amount of power for the boiling point of water at atmospheric pressure.
For this report the assumption is made that $S_l = 1$ and $S_g = 0$, therefore the equation for heat in place can be simplified to:

$$q_r = V\overline{\rho c}(T_R - T_r)$$

Where:

$$\overline{\rho c} = \phi S_l \rho_l c_l + (1-\phi)\rho_r c_r$$

The heat in place of a geothermal reservoir is not the actual heat that can be extracted from a reservoir. This would mean that the recovery reaches a 100% efficiency which is not a reasonable number. Due to characteristics as the reservoir characteristics, structure, and heat loss the recovery is < 100%. For any geothermal reservoir a geothermal recovery factor R_g should be introduced which leads to the following equation for recoverable heat(Garg and Combs, 2015).

$$q_w = R_g V\overline{\rho c}(T_R - T_r)$$

According to 'Williams, 2014' and 'Garg and Combs, 2015' the geothermal recovery factor varies between 0.1 to 0.25 for a sediment hosted reservoir, such as most reservoirs in the Rotliegend formation. To account for the uncertainty in some of the input parameters a probability distribution of the HIP and RH should be made to give insight to the range of expected outcomes. To do so, the values are estimated using Monte Carlo simulations. The number of simulations to produce a good estimate is not yet known but , as there are a lot of uncertainties, the expectation arises that it should be a high number (>1000). From the probability distribution given by the Monte Carlo simulations, the P90, P50, and P10 estimates can also be calculated. Finally, it is important to note that for these calculations the permeability values of the wells in the reservoirs were used. These values could be found in the NLOG database.

3.3. DoubletCalc

For the final step of the reservoir evaluation, DoubletCalc is used. This is an open source software, designed by TNO, which gives an indication to the thermal power output of a geothermal reservoir. This is not the final output of a geothermal power plant as the heat produced still has to be converted to electricity.
The output that Doubletcalc provides is very extensive. besides information on the power production and flow rate it also estimates the pressures, heat loss and COP (ratio between pump production and

consumption). It uses Monte Carlo simulation techniques to come up with the probability distribution. DoubletCalc assumes a geothermal reservoir to be a 'doublet', which has an injector and a producer well, as can be seen in a schematic overview of the model in figure (3.3).

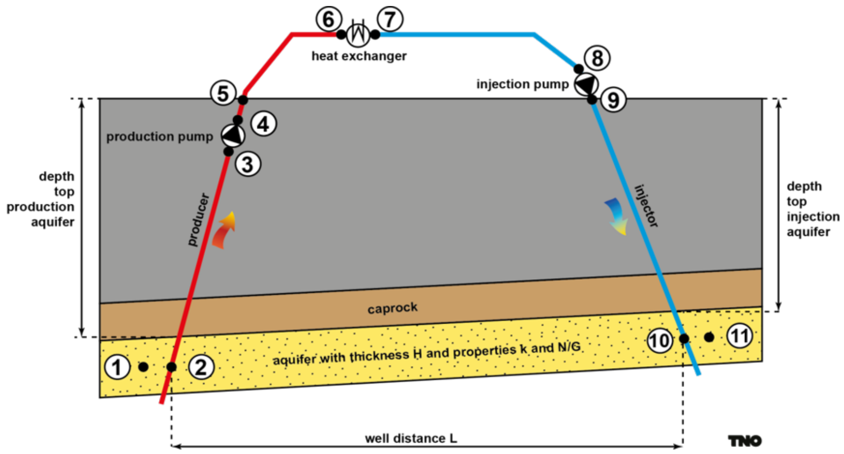

Figure 3.3: schematic drawing of the DoubletCalc model

3.3.1. Governing equations

Doubletcalc estimates the thermal power output ($P_{thermal}$) of a Doublet using the following equation:

$$P_{thermal} = Q_m c_p \Delta T$$

Where:

- $Q_m\,(kg/s)$: Mass flow through the production well
- $c_p\,(kJ/kg°C)$: the heat coefficient of the reservoir fluid at the heat exchanger using known temperature, pressure and salinity.
- $\Delta T\,(°C)$: difference in temperature at the inlet and outlet of the heat exchanger

To solve this equation the temperature loss, and pressure evolution in the well have to be calculated. To do so, first of all the geothermal gradient should be defined, Doubletcalc uses this gradient to estimate the temperature in the aquifer. The aquifer temperatureT_{aq} is defined as follows:

$$T_{aq} = T_{surface} + \lambda(d_{aq} + 0.5H)$$

where:

- $T_{surface}\,(°C)$: the surface temperature, in this case the average North sea temperature
- $\lambda\,(°C/m)$: Geothermal gradient of the reservoir, calculated using data from the SNS temperature database.
- $d_{aq}\,(TVDm)$: the depth of the top of the aquifer
- $H\,(m)$: thickness of the aquifer

The temperature at the inlet of the heat exchanger (location 6 in figure 3.3) has to be calculated by estimating the heat loss in the well and subtracting it from the aquifer temperature. The temperature difference is given by:

$$\frac{dT_{well}}{dl} = \frac{q_{h,well}}{Q_m c_p}$$

where:

- $q_{h,well}\,(W/m)$: heat loss per unit length of the well.

All the equations described in this section are taken from the Doubletcalc manual, (Mijnlieff et al., 2014).

3.3.2. Input properties

There are 3 main properties that have to be defined in the DoubletCalc input window:

- A) Aquifer properties
- B) Doublet and pump properties
- C) Well properties

Figure B.3 in the appendix gives a good overview of all the different inputs. Some of the input variables remain constant for every well. These are all the doublet and pump properties, and the skin factor.

exit temperature at heat exchanger ($^{\circ}C$)	90
distance wells at aquifer level (m)	1500
pump system efficiency (-)	0.8
production pump depth (m)	500
pump pressure difference (bar)	40
skin (-)	0
penetration angle (deg)	0

Table 3.1: Table with an overview of all the constants in the DoubletCalc model

The above pump properties are all assumptions that were made. After the conversion step in the heat exchanger the water is assumed to be around 90° C. For a good Doublet system it is assumed that the distance between the producer well and inlet well is 1500m. A suitable pump for the producer well can reach an efficiency of around 80% (Archer, 2021), with a pressure difference of 50 bar and at 500m depth in the well. As there is no information to be found on the skin on a depleted well, this was assumed to be 0.

The aquifer properties and well properties are yet to be defined, but this be done after the reservoirs of interest have been selected. An overview of the rest of the input data used can be found at the end of the next chapter as the reservoirs of interest have yet to be selected.

4

Results of the Reservoirs Selection Process

This chapter discusses the reservoirs that were selected using the method described in the previous chapter. Additionally, an interpretation of their characteristics such as net to gross ratio, porosity, permeability, and reservoir area are covered. With this information the reservoir evaluation step in the next chapter can also be done.

4.1. Selected reservoirs

In total there was data on 360 different *wells* in the Dutch offshore that showed Rotliegend penetration, from this number only 83 showed a sufficient temperature of $> 120°C$. The wells where then connected to a x,y-coordinate of their location in the Dutch offshore and put in the QGIS model. There the wells were linked to the reservoir they belong to.
These reservoirs were evaluated on their permeability using the interpolated permeability map. The reservoirs that were selected had to contain a region in them where the permeability map showed a permeability higher higher than the previously mentioned threshold of 40 mD. With this information the the preliminary selection could be brought down from 83 wells to only 6 possible reservoirs. These reservoirs are shown in table & figure 4.1.

reservoir name	reservoir code	production wells present
K05-F	K05-F	K05-11
K12-S1	K12-S1	K12-11
K12-S3	K12-S3	K12-16
K15-FB	K15-FB	K15-FB-101, K15-FB-102, K15-FB-103, K15-FB-104, K15-FB-105, K15-FB-106
K15-FG	K15-FG	K15-12, K15-FG-102, K15-FG-103
K15-FK	K15-FK	K15-FK-101, K15-FK-102, K15-FK-105, K15-FK-106

Table 4.1: Overview of reservoirs that belong to the final reservoir selection

The reservoirs shown in the table above have the following characteristics and will be used for a final evaluation based on their reservoir properties:

- **proven** sufficient Temperature ($> 120°$C)
- **proven** gas/oil reservoir
- **(partially)** located in a region of sufficient permeability(>40mD)

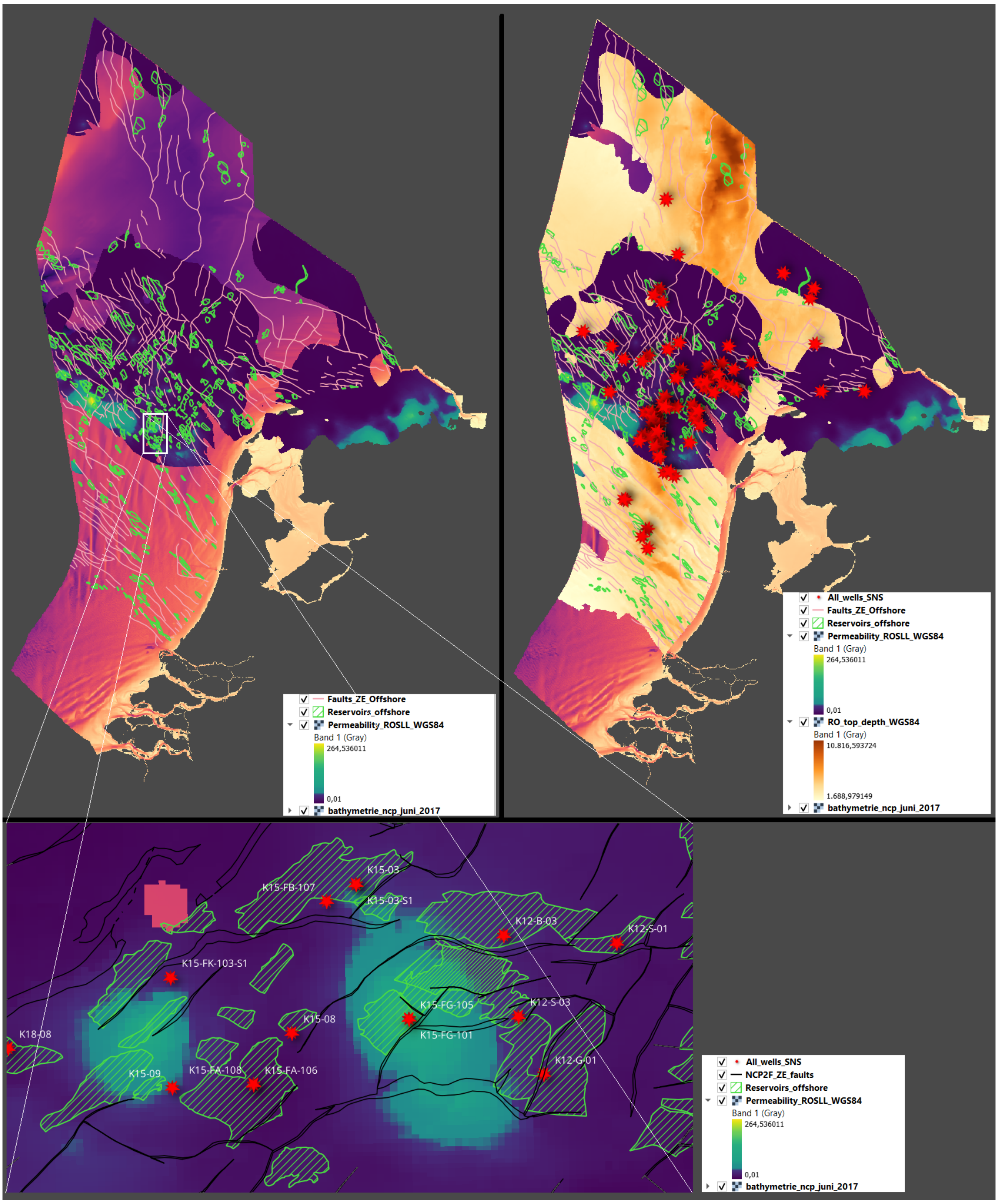

Figure 4.1: **top left:** initial qgis model with information on permeability and faults; **top right:** Wells with sufficient known Rotliegend temperature added, as well as the top of the Rotliegend; **bottom:** Location where it is visible that some reservoirs lay in regions of higher permeability

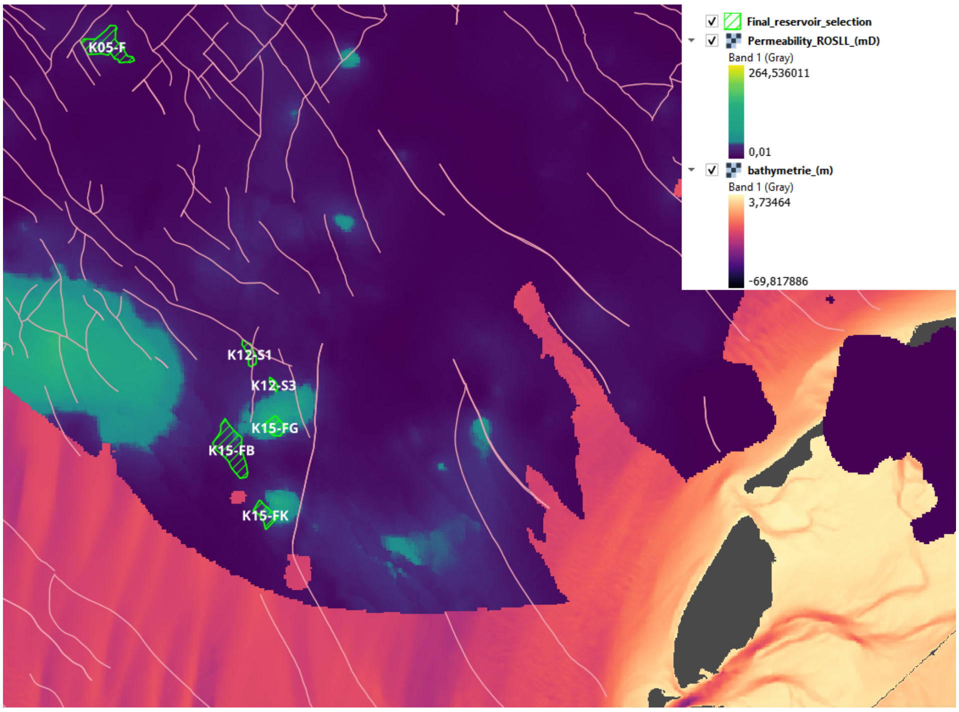

Figure 4.2: Overview of the final selection of reservoirs that showed an adequate temperature and permeability

The selected reservoirs after permeability evaluation are all Gas reservoirs. Five of them lay relatively close together (<20km), as can be seen in figure 4.2. These are the reservoirs laying in the K15 and K12 block. The final step is to look at the proximity of these reservoirs to existing electricity infrastructure of the dutch offshore. From figure 4.2 we can already see that the K15, and K12 reservoirs all lay in the same area. The exception here is reservoir K05-F, which lays double the distance away from the Dutch offshore as the other reservoirs. In figure B.6 of the appendix it can also be seen that coincidentally, the four of the five reservoirs in the K12, and K15 block, lay exactly in a wind farm development area. The exception here is reservoir K15-FK which lays just outside of the development area, but not far enough to disregard in the reservoir evaluation step. This is not the same for reservoir K05-F, that is 50 km away from the wind farm development area that the other the other reservoirs belong to. The cost of constructing electricity cables on the seafloor is estimated between €220,000 and €2,500,000 (Ruijgrok et al., 2019) for minor and major cables. Making it much more interesting to look at the reservoirs already in the wind farm development area.

4.2. Characteristics and geometry of selected reservoirs

To determine the volumetric size of the reservoirs, the coverage area and thickness of the reservoirs are needed. First of all the area per reservoir should be determined, although this can easily be computed by calculating the area per reservoir in QGIS, it overlooks the fact that these reservoirs based on the Gas Water Contact (GWC). In figure 4.4 and 4.5, the GWC line is given for reservoirs K15-FK and K15-FB.

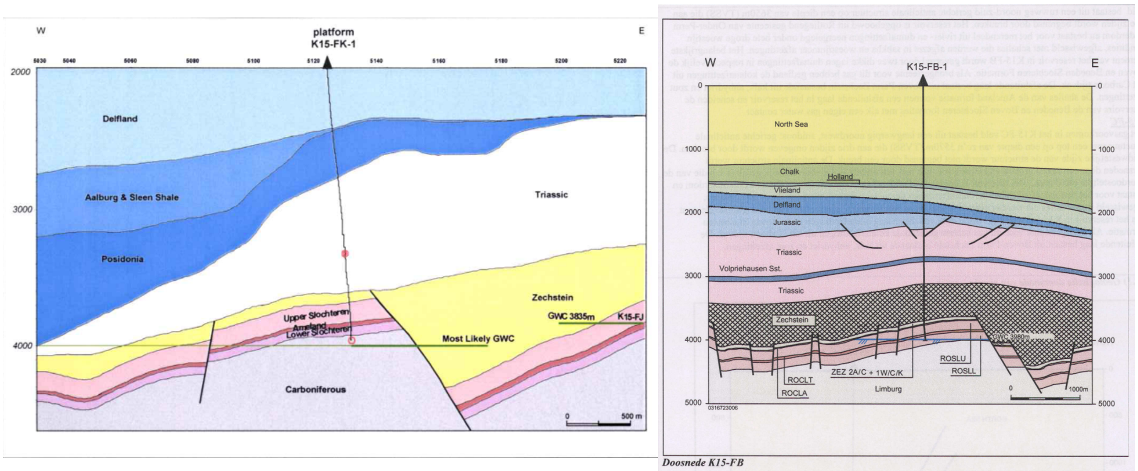

Figure 4.3: Cross section West to East of reservoir K15-FK (left) and reservoir K15-FB (right)

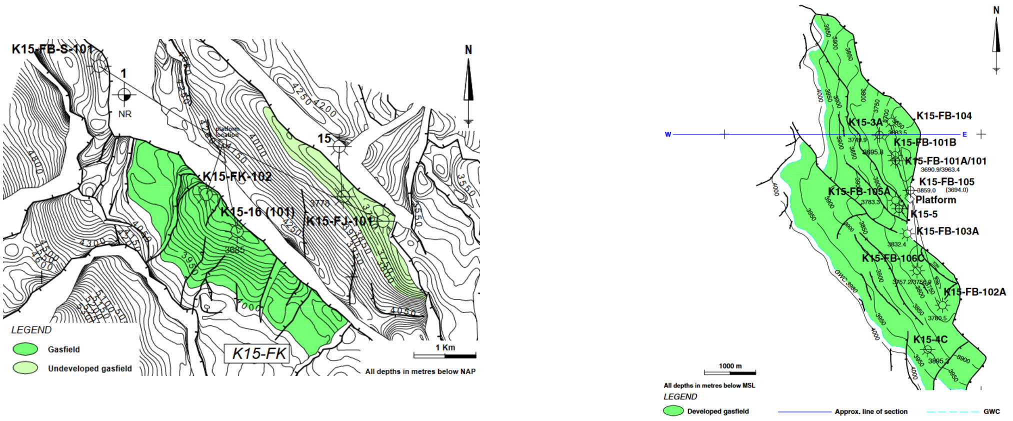

Figure 4.4: Top view of reservoir K15-FK (left) and K15-FB (right) where the green area marks the reservoir based on the GWC

This GWC is used for the reservoir outlines, as can be seen in figures 4.6 and 4.7. Gas sits on top of the fluid the geothermal reservoir could be much larger than is shown in the figures below. Therefore for a new outline is proposed for the reservoirs based on the faults visible in the structure maps. As it is unknown how the fault affects the permeability next to it, it is assumed that the faults impose an barrier for the aquifer during production. Therefore the newly proposed reservoir outline will is selected by looking at the areas of the reservoir that are in contact without any faults cutting through it. An example of this is given in figure 4.8 where the red line proposes the new reservoir that can be viewed as one piece, not cut by faults. The original reservoir (green accentuated area) is partially fully cut by one fault, therefore the smaller part is left out.

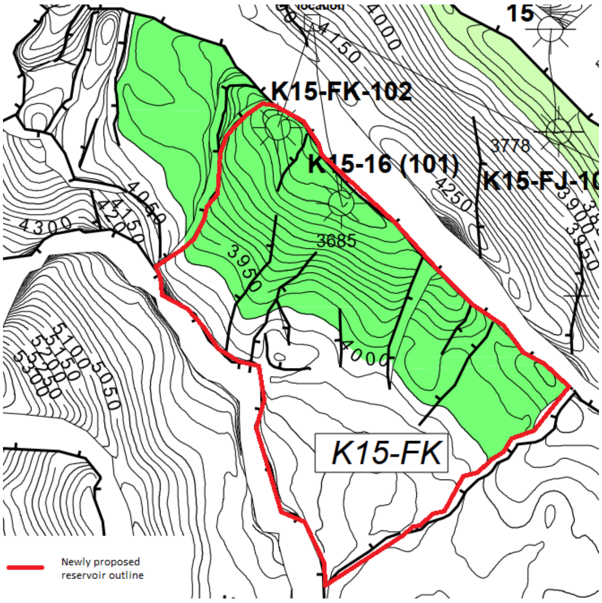

Figure 4.5: Newly proposed geothermal reservoir based on Top view structure (faults) and the cross section

This approach was used for all the selected reservoirs, resulting in the following new estimates:

reservoir	gas reservoir area (m^2)	new proposed aquifer area (m^2)
K12-S1	2297385	3047055
K12-S3	968581	956777
K15-FB	5751621	16760947
K15-FG	3772043	4631912
K15-FK	4253890	4998992

Table 4.2: Comparison between the old and the new reservoir area

4.3. Aquifer properties

The properties of the selected reservoirs were obtained using the publicly available data on NLOG and the SNS database. The gross thickness, and net to gross thicknesses of the reservoirs were obtained by analyzing the gamma-ray API of the composite well logs from the reservoir wells.
The data on the reservoir porosity and permeability that was publically available, was unfortunately very limited. Often only 10-20% of the full reservoir had porosity and permeability measurements. This makes both the average porosity and permeability a rough approximation of the actual values of the reservoir.
Finally the geothermal gradient per reservoir was calculated using the available temperature data fro the SNS database.

reservoir	Thicknesses (m)			NTG (-)	permeability (mD)			geothermal grad (°C)
	min	median	max		min	median	max	
K12-S1	284	285	287	0.56	0.47	12	595	29.8
K12-S3	302	305	311	0.42	0.03	0.55	1100	30.8
K15-FB	286	295	303	-	-	-	-	-
K15-FG	314	314.2	317	0.51	0.01	0.93	189	31.9
K15-FK	331	326	336	0.64	0.02	3.81	884	33.7

Table 4.3: Table with overview of some important parameters that are used for heat in place estimations, and DoubletCalc simulations

First of all we can observe that well K15-FB does *not* have any measured porosity or permeability values. Therefore this, just like K05-F, reservoir is also disregarded for final evaluation.

It is important to mention that the above porosity and permeability values are the *initial* porosity and permeability measurements, and are not adjusted to the increased compaction rate due to reservoir depletion. As the pressure of the hydrocarbons in the pores decreases the reservoir is compacted leading to decreases in porosity and permeability (Belhaj and Nouri, 2007), altough permeability seems to be less effected. To what extend this impacts the reservoirs in this study is hard to predict because 1): during depletion only gas is extracted from the reservoir and since this only takes place in the gas bearing part of the reservoir, water remains in the lower parts of the reservoir. 2): During gas extraction the pressure in the gas bearing part of the reservoir, therefore water migrate into the emptied pores in the depleted part. To what extend this takes is very hard to say, no references could be found on this matter.
Nevertheless, some decrease in porosity and possibly also permeability takes place which should be mentioned in the discussion and conclusion.

The salinity of the Rotliegend layer is quite high, the reason for this is partially the deposition facies which may have contained layers of evaporites that made the aquifer saline, but mainly this is caused by the Zechstein evaporites layer that is the reservoir seal. Over many year the aquifer water became highly saline due to contact with this layer (Lüders et al., 2010). The salinity at the different reservoirs is estimated from figure 9 of 'Verweij et al., 2011'. An uncertainty of 25,000 ppm is assumed as it is hard to see where exactly the selected reservoirs lay in figure 9 of 'Verweij et al., 2011'.

The ratio between horizontal and vertical permeability (kv/kh) is important to consider for the flow between layers in the reservoir. Due to vertical heterogeneity in the reservoir formation, the vertical permeability can be considerable smaller than the horizontal permeability. The vertical permeability ranges from 0.01 to 1 times the horizontal permeability (Tichler et al., 2016). The Vertical Permeability is computed from the Permeability values from well K12-S3 as this was the only reservoir that also had vertical permeability estimates. The ratio between kh/kv = 5.46 (in terms of kv/kh equal to 0.18), for lower Slochteren formation. This ratio is kept constant for the other reservoirs too.
The surface temperature is kept at a constant of 12.5 degrees Celsius, which is also the approximate average yearly north sea temperature ("Sea water temperature", 2023).

reservoir	salinity (ppm)		
	min	med	max
K12-S1	225,000	250,000	275,000
K12-S3	235,000	260,000	295,000
K15-FG	275,000	300,000	325,000
K15-FK	250,000	275,000	300,000

Table 4.4: Overview of some aquifer properties

5
Evaluation of Selected Reservoirs

In this chapter the five reservoirs that were selected in the previous chapter are evaluated. An indication of their geothermal potential is given, based on their heat in place, and approximate power output. First the heat in place and recoverable heat are discussed, after which the flow rate and power output computed with Doubletcalc are presented. Using this information recommendations on the technical potential of the reservoirs can be given.

5.1. Reservoir properties and recoverable heat

The first step was to calculate the estimated HIP q_r, and RH q_w from the reservoirs. Some of the inputs that were used for calculating the HIP and RH are shown in table **??**.The results of the HIP and RH estimates through Monte Carlo simulation are shown in table 5.1, with an example of the distributions presented in figure 5.1 on the next page.

reservoir	HIP (10^{15} J)			RH (10^{15} J)		
	P90	P50	P10	P90	P50	P10
K12_S1	13.911	15.221	16.617	0.352	1.864	3.429
K12_S3	6.479	7.366	8.359	0.187	0.919	1.659
K15_FG	20.886	22.828	24.88	0.563	2.77	5.136
K15_FK	41.804	45.231	48.856	1.159	5.672	10.087

Table 5.1: Overview of the heat in place and recoverable heat distributions using Monte Carlo simulations

With a reference temperature of 100° C, the max heat in place is in the range of 10^{17} J which seems a reasonable value based on comparison to other geothermal reservoirs.

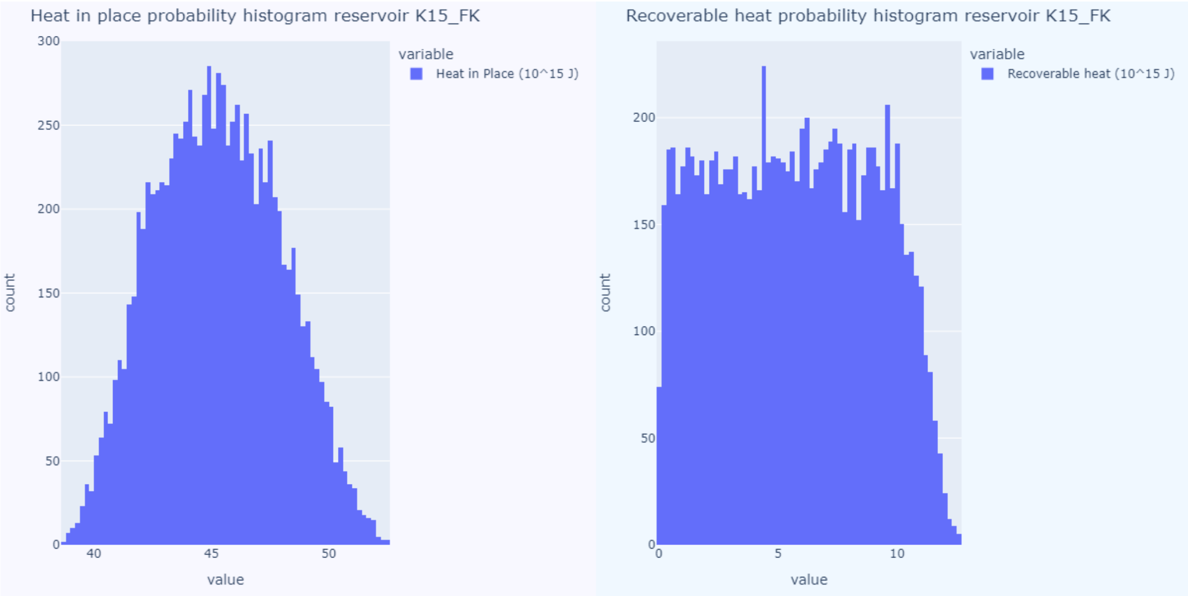

Figure 5.1: Estimated Heat in place and Recoverable heat by using 10,000 Monte Carlo simulations

The Python code that was used to calculate the above presented values can be found in appendix A.

5.2. Reservoir performance estimation

In the Doubletcalc model it is important to define some variables so that the simulations can be performed. These variables are kept constant for all reservoirs so that an even comparison can be made. The rest of the variables that have not been defined in the previously defined tables (4.3 & 4.4), are dependent of the reservoir wells and cannot be considered to be constant per scenario.
The data on the reservoir wells such as the roughness in the pipes, diameter of the pipes and the length of the pipe segments could be found in the files from ("NLOG", 2023). Using all of this data the following results were obtained for the estimated thermal power if a doublet system would be built.

reservoir	pump volume flow (m3/h)			average thermal power output (MW)		
	P90	P50	P10	P90	P50	P10
K12-S1	12.56	27.58	169.82	-0.11	0.51	6.45
K12-S3	0.49	2.62	183.36	-0.7	-0.1	7.71
K15-FG	1.03	2.36	94.89	-0.13	-0.04	3.97
K15-FK	6.71	14.66	189.05	-0.16	0.19	11.02

Table 5.2: Overview of final results from Doubletcalc

Unfortunately the thermal power output is low (<1MW for the median scenario) for all reservoirs, as can be seen in table 5.2. The reason for these extremely low values most likely has to do with the fact that the median measured permeabilities are very low in all the reservoirs. From table 4.3 it can be observed that the minimal and median values are all in between 0.01 and 12, while the maximum value is much higher. This trend can be observed when looking at figures 5.2a & 5.2b, where this is the same case: P90 and P50 are close together while P10 is much higher.

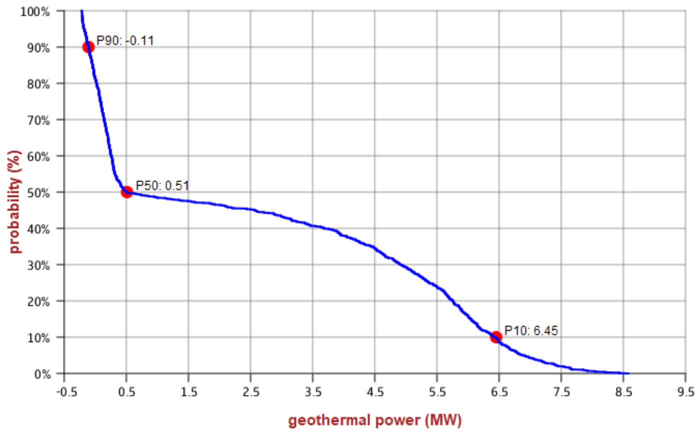

(a) result of estimated thermal power output

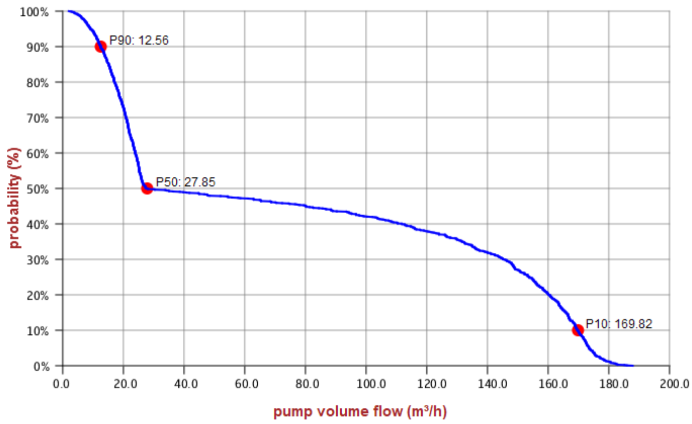

(b) results of estimated pump volume

Considering that the thermal energy still has to be converted into electricity the outcome is expected to be very low. For a low-temperature geothermal systems, a binary power plant is most often used (Sharmin et al., 2023). Such a plant is able to convert around 40% of the thermal energy into electricity, altough considering that the plant also uses energy, the efficiency is reduced to about 14% (Colpan et al., 2021). This means that for instance reservoir K12-S1, the reservoir that showed the best median permeability, only generates about 0.51 MW of electricity.

6 Discussion

For obtaining the results presented in the previous chapter a lot of assumptions had to be made. First of all with the reservoir selection process. The temperature data for the wells in the SNS database only contained a limited number of temperature data points per well. Therefore, during the filtering process a number of reservoirs could have been been filtered out as their maximum formation temperature was not sufficient. This can happen when the data point with the maximum temperature is encountered high up in the reservoir. Additionally the permeability map used from NLOG in QGIS, that was one of the main components to the reservoir selection step, was a mapped obtained by interpolation from known datapoints. Therefore this map did not give a representable view of the permeability. This statement is enforced by the fact that a reservoir formation, such as the ROSLL, varies a lot in vertical direction. Alternating between shale and sandstone layer.

For the reservoir evaluation process the assumption was made that the reservoir was a homogeneous, isotropic reservoir. This assures that all the properties of the reservoir are equal towards all directions. This again misses the fact that the reservoir layers are made up of alternating layers of shale and sandstone. On top of that the shaley Laapakket of Ameland, separates the Boven- and Onder-Slochteren formations (“Dinoloket”, 2023). Making it hard to know if the layers are hydraulically connected.
The shape of the reservoir too remains an unsure parameter as this has only been based on the available structure maps, and cross section per reservoir.

With regards to the reservoir evaluations also a lot of uncertainties are present. The temperature loss for instance, does not take into account the existence of a water column in the final <100m. It is therefore unknown how great the heat loss will be as 1): the sea water temperature fluctuates between $\pm 5°C$ in the winter and $\pm 20°C$ during the summer “Sea water temperature”, 2023, and 2): Water has a higher heat capacity than rock and will therefore transport heat more easily. Altough it is assumed that some insulation will be added to the well in the water column, its effects are unknown.
Additionally, the outlines of the reservoirs are based on faults and top depths of the Rotliegend. The faults are assumed to be barriers to the reservoir but this would then also mean that the influx of water during reservoir depletion is uncertain.
Finally, the porosity and permeability measurements are also not valid for the full reservoir layer as they only cover about 10-20% of the whole reservoir layer. Therefore these values are merely a ’snapshot’ of the full reservoir porosity, and permeability.

Looking back at the research done, steps taken and eventual outcome lead to the idea that the method of reservoir selection can be disputed, some reservoirs show better permeability and are still found at depths of >3500m but do not belong in the final selection of reservoirs. This in known as the author also looked at reservoirs that were not recommended during the selection process. As the geothermal gradient remains quite constant through the subsurface it might have been better to only look at all the high permeability reservoirs from the QGIS map and evaluate them using the approximate known geothermal gradient ($\pm$ 31°C).

7
Conclusion

The objective of this report was to assess if hydrocarbon reservoirs in the Dutch offshore could be reused for geothermal projects. A combination of a lot of available reservoir data and good geological knowledge of this region made it an interesting option. The two main questions of the report were 1): which reservoirs in the Dutch offshore look good on paper for development of geothermal electricity production and 2): what is their technical potential based on the data available?

To do so, first the 'best' reservoirs were chosen based on their temperature and permeability. This left us with 6 reservoirs that showed the highest potential: K05-F. K12-S1, K12-S3, K15-FB, K15-FG, and finally K15-FK, which answers the first research question.
Due to location and lack of *measured* permeability values reservoirs K05-F and K15-FB had to be disregarded from the final step: assessing the previous selected reservoirs on their technical potential. The estimated amount of resources present in the reservoirs was quite high (10^{17} J), suggesting that the reservoirs could be interesting geothermal energy production.
This idea was unfortunately changed with estimating the thermal power output of the well using DoubletCalc. The 4 wells that were evaluated during this step all showed a extremely low thermal power output of <1 MW. As the thermal energy also has to be converted into electricity, the reservoirs were not suitable for generating electricity.

As these reservoirs were the reservoirs with the highest potential, as stated earlier, the expectation is that all the dutch offshore hydrocarbon reservoirs are *not* suitable to reuse for geothermal electricity projects. The reason for this being the low power output associated with the reservoirs. The reason for this has to do with the permeability of the layers. Altough the permeability maps in QGIS suggested that the permeability in the reservoirs could be around 40mD, the measured median permeability value was 12mD for reservoir K12-S1. As large parts of the Rotliegend in the Dutch offshore has been inverted, permeability values could be much lower than expected for these depths, resulting in these disappointing results.

8 Recommendations

This report was written on request of the geothermal department of Witteveen+Bos, therefore the following recommendations are given on the subject.

The geothermal electricity production potential in the Dutch offshore is very limited when reusing hydrocarbon reservoirs for this purpose. This comes mainly down to the fact that the permeability in these reservoirs is too low for a production rate that makes the such a project economically interesting. There are some nuances to this conclusion that should be investigated further:

- As stated in the discussion the method of selecting the reservoirs was based on known temperatures, but also interpolated permeability values. One of the problems encountered was that of all the reservoirs in the Dutch offshore did not all have wells of which data was stored in the SNS database. Therefore some reservoirs might have been disregarded from the selection procedure before assessing them with the permeability maps. Therefore one can also look *just* at the permeabilities and afterwards estimating the reservoir temperatures.
- The data used for this project, especially relating to the measured porosity and permeability values from NLOG covered only a small part of the reservoirs. Therefore the power output is only a rough estimation as it is unknown what the permeability in the full reservoirs looks like. This should be requested from the operators of the reservoirs, as expanding the life-expectancy of a reservoir & platform could be interesting for them aswell.
- This report only assumes the reservoir to be reused without any modifications to the permeability. This relates to option of 'fracking' a reservoir to artificially increasing the technical potential.

Taking into account these points could lead to a different conclusion when investigating offshore geothermal energy production. Nevertheless I want to emphasize that the permeability values will be a severe limitation to such a project and one should expect that even with EGS, the capacity might be limited.

References

Archer, C. (2021). *How to calculate (and improve) pump efficiency* [date accessed: 26-10-2023]. https://blog.wellaware.us/blog/how-to-calculate-pump-efficiency

Aydin, H., & Merey, S. (2021). Potential of geothermal energy production from depleted gas fields: A case study of dodan field, turkey. *Renewable Energy*, *164*, 1076–1088. https://doi.org/https://doi.org/10.1016/j.renene.2020.10.057

Barton, W. (1984). Tectonic evolution of the north sea basin: Crustal stretching and subsidence. *Geophysical Journal International, Volume 79, Issue 3, Pages 987–1022*, *79*, 987–1022.

Belhaj, H., & Nouri, A. (2007). Reservoir rock behavior pre and post pore collapse during production. https://doi.org/10.2523/IPTC-11657-MS

Colpan, C., Ezan, M., & Kizilkan, O. (2021). Thermodynamic analysis and optimization of geothermal power plants. Elsevier. https://doi.org/https://doi.org/10.1016/B978-0-12-821037-6.09995-9

de Jager, J. (2007). Geological development. *Geology of the Netherlands*, 5–26.

Dinoloket [date accessesd: 11-09-2023]. (2023).

Editors of Encyclopaedia Britannica. (2020, January). *Alluvial deposit* [https://www.britannica.com/science/alluvial-deposit]. Encyclopedia Britannica.

Garg, S. K., & Combs, J. (2015). A reformulation of usgs volumetric "heat in place" resource estimation method. *Geothermics*, *55*, 150–158. https://doi.org/https://doi.org/10.1016/j.geothermics.2015.02.004

Geode atlas [date accessed: 20-09-2023]. (2023). https://www.geodeatlas.nl/pages/about

Guzović, Z., Lončar, D., & Ferdelji, N. (2010). Possibilities of electricity generation in the republic of croatia by means of geothermal energy. *Energy*, *35*(8), 3429–3440. https://doi.org/https://doi.org/10.1016/j.energy.2010.04.036

Kabeyi, M. (2019). Geothermal electricity generation, challenges, opportunities and recommendations. *International Journal of Advances in Scientific Research and Engineering*, *5*. https://doi.org/10.31695/IJASRE.2019.33408

Kortekaas, M., Böker, U., van der Kooij, C., & Jaarsma, B. (2018). Lower triassic reservoir development in the northern dutch offshore. *Geological Society, London, Special Publications*, *469*(1), 149–168. https://doi.org/10.1144/SP469.19

Lüders, V., Plessen, B., Romer, R. L., Weise, S. M., Banks, D. A., Hoth, P., Dulski, P., & Schettler, G. (2010). Chemistry and isotopic composition of rotliegend and upper carboniferous formation waters from the north german basin. *Chemical Geology*, *276*(3), 198–208. https://doi.org/https://doi.org/10.1016/j.chemgeo.2010.06.006

Mahtab, M., Peter, G., Alberto, R., Kees, G., Joanna, G., & Julie, D. (2019). *Facies analysis and diagenetic evolution of the dinantian carbonates in the dutch subsurface* (tech. rep.). SCAN. https://www.nlog.nl/sites/default/files/2019-09/scan_dinantian_facies_analysis_and_diagenetic_evolution_of_the_dinantian_carbonates_in_the_dutch_subsurface.pdf

Mckie, T. (2011). A comparison of modern dryland depositional systems with the rotliegend group in the netherlands. *SEPM Special Publications*, *98*, 89–103. https://doi.org/10.2110/pec.11.98.0089

Moeck, I. (2014). Catalog of geothermal play types based on geologic controls. *Renewable and Sustainable Energy Reviews*, *37*, 867–882. https://doi.org/10.1016/j.rser.2014.05.032

Nlog [data accessed: 11-09-2023]. (2023). https://www.nlog.nl/

of US Department of energy, A. (2023). *Enhanced geothermal systems*. https://www.energy.gov/eere/geothermal/enhanced-geothermal-systems

Ruijgrok, E., van Druten, E., & Bulder, B. (2019). *Cost evaluation of north sea offshore wind post 2030* (tech. rep.). North Sea Wind Power Hub Consortium.

Salameh, Z. (2014). Chapter 5 - emerging renewable energy sources. In Z. Salameh (Ed.), *Renewable energy system design* (pp. 299–371). Academic Press. https://doi.org/https://doi.org/10.1016/B978-0-12-374991-8.00005-2

Sea water temperature. (2023). NIOZ. https://www.nioz.nl/en/expertise/wadden-delta-research-centre/data-tools/long-term-ecological-time-series/sea-water-temperature

Sharmin, T., Khan, N. R., Akram, M. S., & Ehsan, M. M. (2023). A state-of-the-art review on geothermal energy extraction, utilization, and improvement strategies: Conventional, hybridized, and enhanced geothermal systems. *International Journal of Thermofluids*, *18*, 100323. https://doi.org/https://doi.org/10.1016/j.ijft.2023.100323

Thermogis [data accessed: 26-10-2023]. (2023). TNO. https://www.thermogis.nl/aquifereigenschappen

Tichler, A., Abdulah, S., Haworth, S., van der Wal, O., Hamood, A., Seubring, J., & Barber, S. (2016). *Dynamic reservoir modelling of wadden fields for subsidence* (tech. rep.). NAM B.V.

Mijnlieff, H., Obdam, A., van Wees. J.D.A.M, Pluymaekers, M., & Veldkamp, J. (2014). *Doubletcalc 1.4 manual english version for doubletcalc 1.4.3*.

Van Hulten, F. (2006). Reservoir quality distribution as tool for better exploration prospect evaluation and estimation of the resource base in the netherlands.

van Gils, H., de Jager, J., & Vinci, F. (2020). *De mogelijkheden en potentie om aardwarmte op te schalen vanuit een ondergrond perspectief* (tech. rep.). EBN, Pantera, Berenschot.

Verweij, J., Simmelink, H., & Underschultz, J. (2011). Pressure and fluid flow systems in the permian rotliegend in the netherlands onshore and offshore. *Society for Sedimentary Geology Special Publication*, *98*, 247–263. https://doi.org/10.2110/pec.11.98.0247

Williams, C. (2014). Evaluating the volume method in the assessment of identified geothermal resources. *Geotherm. Resour. Counc. Trans.*, *38*, 967–974.

A

Python code

Heat in place and recoverable heat estimates

```
import numpy as np
import pandas as pd
import matplotlib
import plotly.express as px
import plotly.graph_objects as go
import matplotlib.pyplot as plt

#Create a df to add the computed values to
df_HIP_RH = pd.DataFrame(columns=['Reservoir','HIP P90 (10^15 J)','HIP P50 (10^15 J)','HIP P10 (10^15 J)','RH P90 (10^15 J)','RH P50 (10^15)','RH P10 (10^15)'])

#create a function that plots the HIP and RH cumulativa, and histogram plots
def hist_plotly(iterations,HIP,RH,factn,res):
    ######Create a histogram of the HIP
    HIP = pd.DataFrame(HIP,columns=[f'Heat in Place ({factn} J)'])
    fig = px.histogram(HIP,nbins=100, width=600, height=600,
                        title=f'Heat in place probability histogram reservoir {res}',)

    fig.update_layout(margin=dict(l=20, r=20, t=40, b=20),
                                paper_bgcolor="ghostwhite")
    fig.show()

    ######Create cumulative distribution of the HIP
    H_HIP, X1_HIP = np.histogram(HIP,bins=100)
    F1_HIP = np.cumsum(H_HIP)/iterations

    dict1 = {f'x {factn}':X1_HIP[1:],'y':F1_HIP}
    data = pd.DataFrame(dict1)
    fig = px.line(data,x=f'x {factn}',y='y',
                  width=600,
                  height=600,
                  title=f'Cumulative HIP distribution of reservoir {res}')
    fig.show()

    ######Create a histogram of the RH
    RH = pd.DataFrame(RH,columns=[f'Recoverable heat ({factn} J)'])
    fig = px.histogram(RH,nbins=100, width=600, height=600,
                        title=f'Recoverable heat probability histogram reservoir {res}',)

    fig.update_layout(margin=dict(l=20, r=20, t=40, b=20),
                                paper_bgcolor="aliceblue")
    fig.show()

    ######Create cumulative distribution of the RH
    H_RH, X1_RH = np.histogram(RH,bins=100)
    F1_RH = np.cumsum(H_RH)/iterations

    dict1 = {f'x {factn}':X1_RH[1:],'y':F1_RH}
```

```
    data = pd.DataFrame(dict1)
    fig = px.line(data,x=f'x {factn}',y='y',
                  width=600,
                  height=600,
                  title=f'Cumulative RH distribution of reservoir {res}')
    fig.show()

    return F1_HIP,F1_RH

#create a function to save the computed values to the dataframe created earlier
def save_to_df(HIP,RH,res,df):
    HIP_P90 = np.round(np.percentile(HIP,10),3)
    HIP_P50 = np.round(np.percentile(HIP,50),3)
    HIP_P10 = np.round(np.percentile(HIP,90),3)

    RH_P90 = np.round(np.percentile(RH,10),3)
    RH_P50 = np.round(np.percentile(RH,50),3)
    RH_P10 = np.round(np.percentile(RH,90),3)

    df.loc[len(df.index)] = [res,HIP_P90,HIP_P50,HIP_P10,RH_P90,RH_P50,RH_P10]
    return df

#Monte Carlo simulation of the reservoirs
def heat_in_place(iterations,Area,Reservoir_top,Reservoir_bottom,Geothermal_gradient,G_range,
    NTG_range,Por_range,res):
    #Define the global constant
    fact =10**15
    factn = '10^15'
    T_r = 100
    dens_liquid = 1050  #kg/m^3
    dens_rock = 2650    #kg/m^3
    q_coef_liquid = 3850 #
    q_coef_rock = 780

    ##Define the reservoir specific constants
    A = Area
    T_R = np.average(np.array([Reservoir_top*Geothermal_gradient,Reservoir_bottom*
        Geothermal_gradient]))
    print(T_R)
    ###Create a list to store the heat in place and recoverable heat values
    HIP = []
    RH = []
    ####Calculate!
    for i in range(0,iterations):
        Gross = np.random.randint(G_range.min(),G_range.max())
        NTG = (np.random.randint(NTG_range.min(),NTG_range.max()))/100
        Por = (np.random.uniform(Por_range.min(),Por_range.max()))/100
        R_w = np.random.uniform(0.1,0.25)

        q_r = (A*Gross*NTG*((Por*dens_liquid*q_coef_liquid)+((1-Por)*dens_rock*q_coef_rock))
            *(T_R-T_r))/fact
        q_w = q_r*R_w

        HIP.append(q_r)
        RH.append(q_w)
        ##Cumulative distribution

    hist_plotly(iterations,HIP,RH,factn,res)

    save_to_df(HIP,RH,res,df_HIP_RH)

    #Calculate some statistics HIP
    mean = np.round(np.mean(np.array(HIP)),3)
    print(f"the mean HIP ={mean}*{factn} J")
    standard_deviation = np.round(np.std(np.array(HIP)),4)
    print(f'the standard deviation of the HIP ={standard_deviation}*{factn} J')

    #Calculate some statistics RH
    mean = np.round(np.mean(np.array(RH)),3)
    print(f'the mean RH ={mean}*{factn} J')
    standard_deviation = np.round(np.std(np.array(RH)),4)
```

```
    print(f'the standard deviation of the RH ={standard_deviation}*{factn} J')

    return df_HIP_RH

#Save the file to an excell file!
df_HIP_RH.to_excel('output/HIP_RH_distributions.xlsx')
```

B

Relevant figures

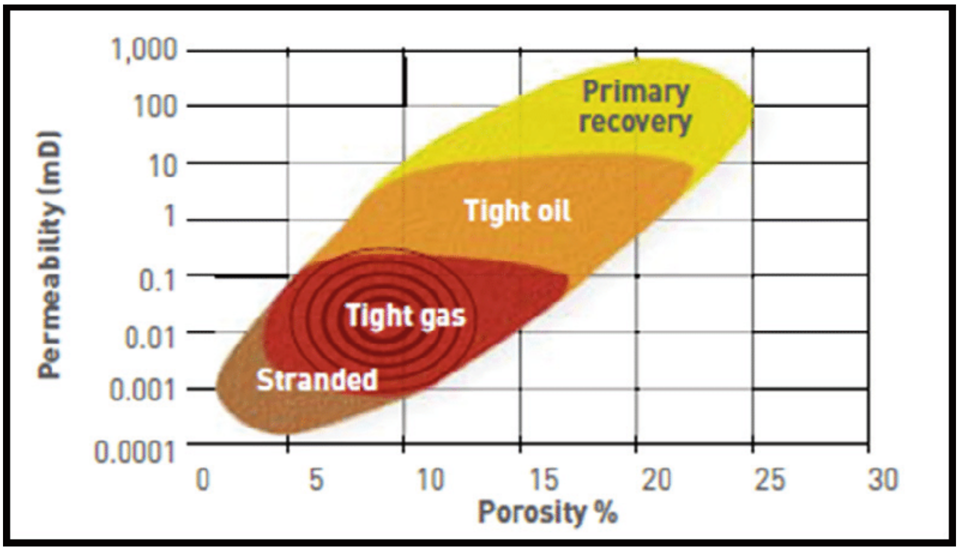

Figure B.1: Porosities and permeabilities associated with tight hydrocarbon reservoirs

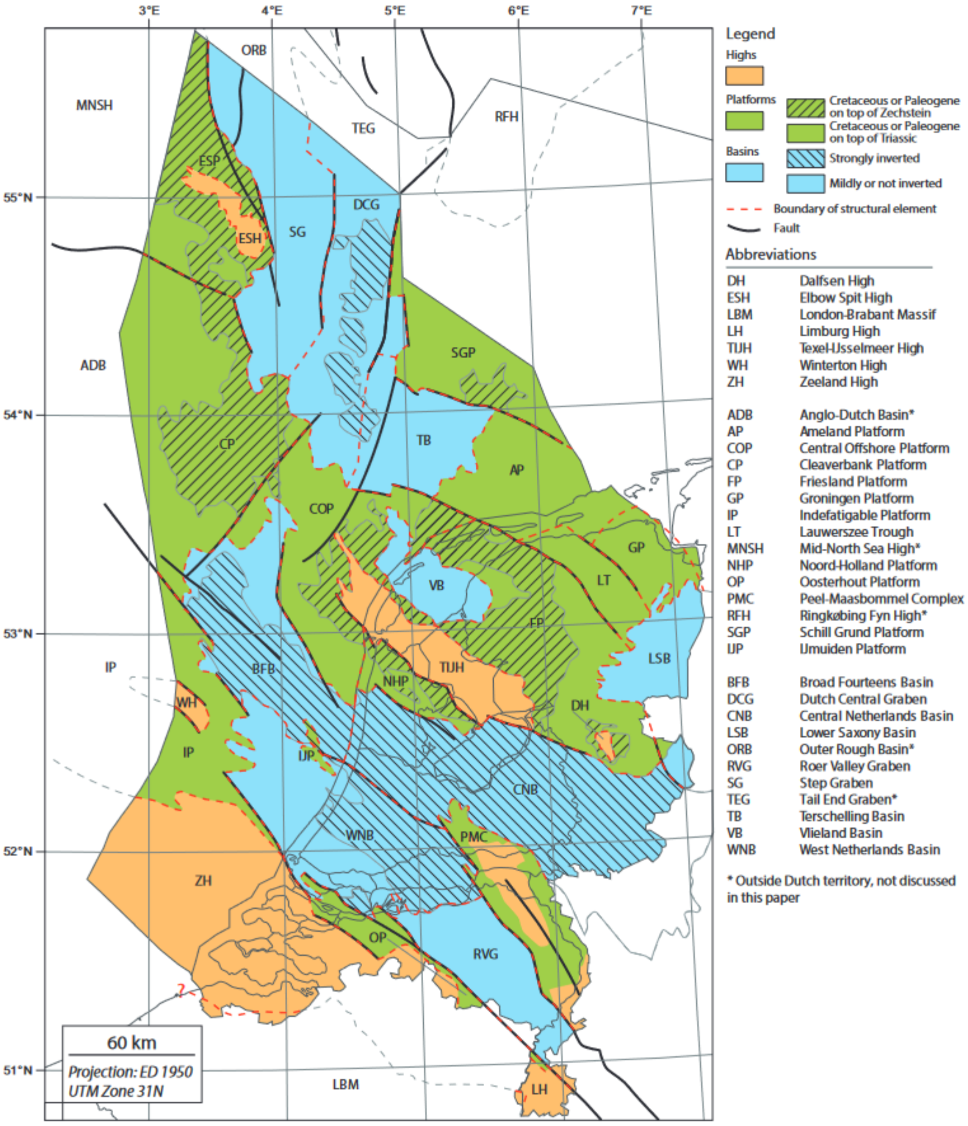

Figure B.2: Inversion in the SNS Basin

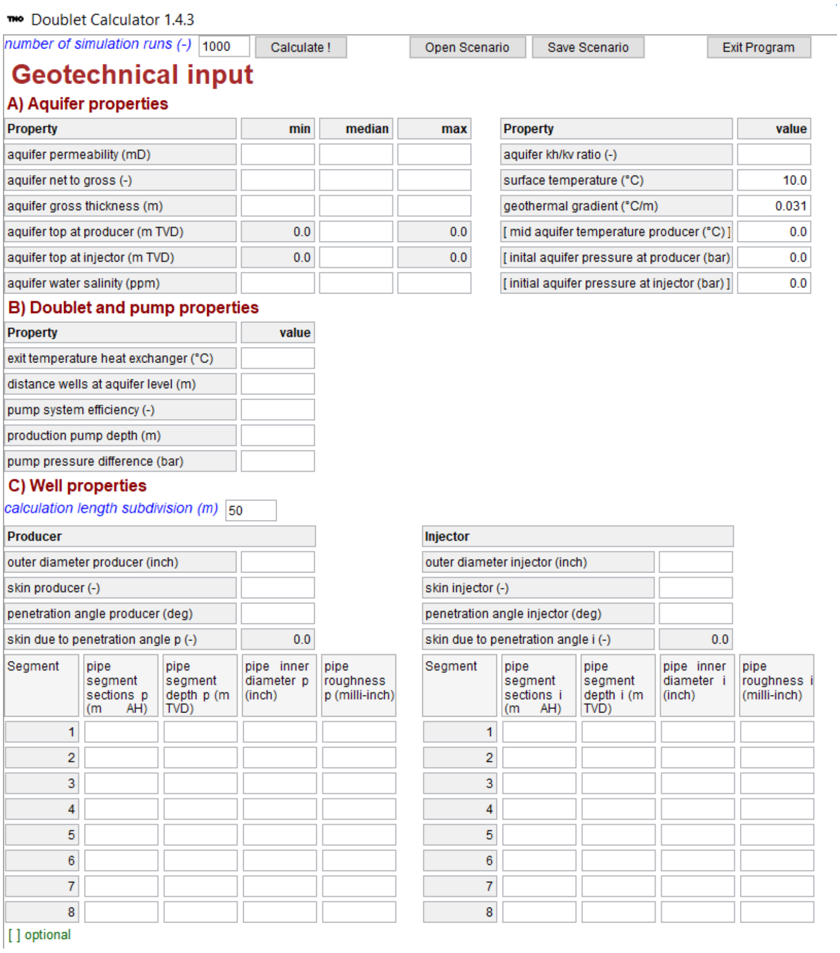

Figure B.3: Input window of Doubletcalc

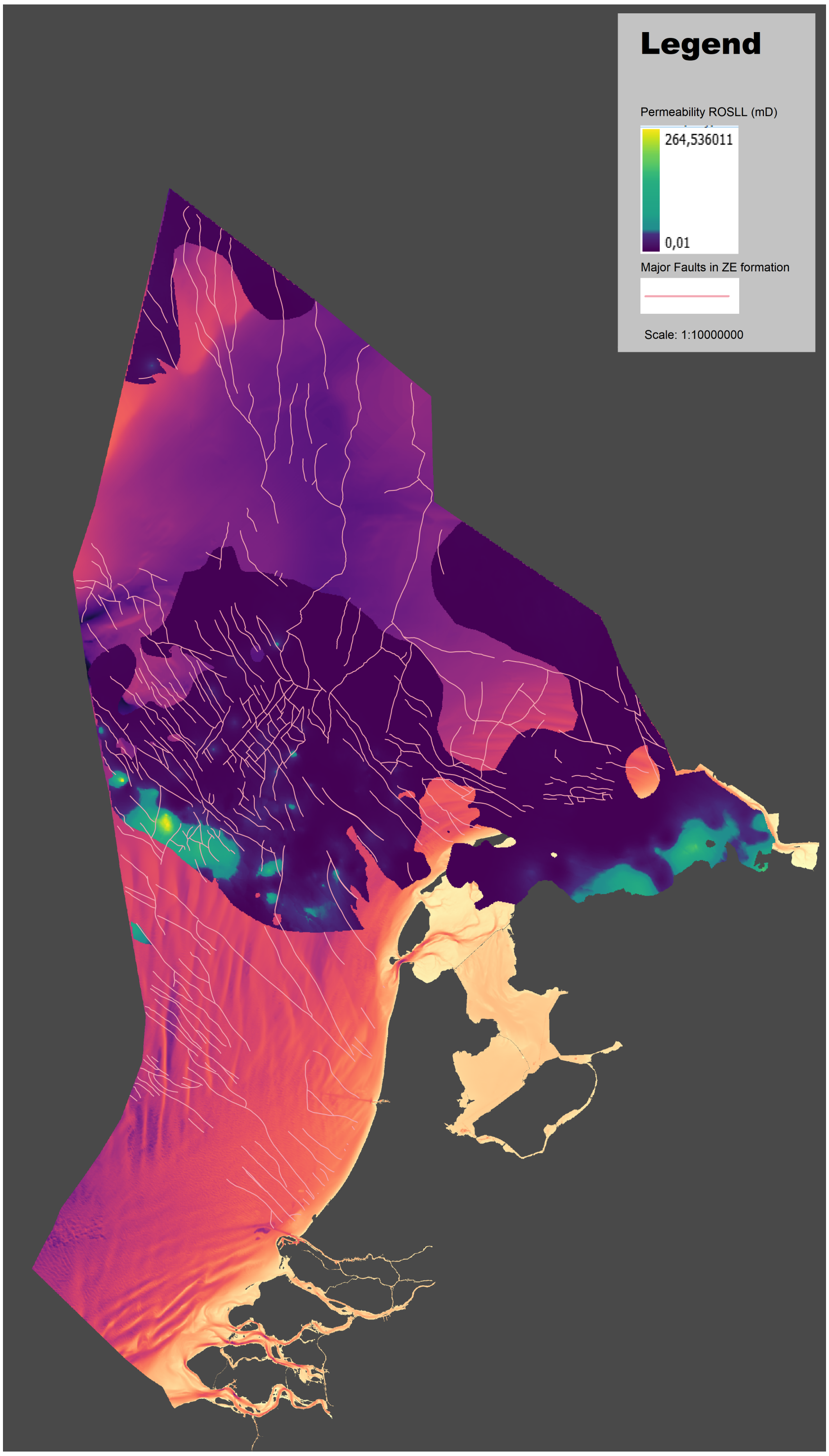

Figure B.4: QGIS model of the dutch offshore with the interpolated permeability of the ROSLL (Onder-Slochteren) formation and major faults displayed

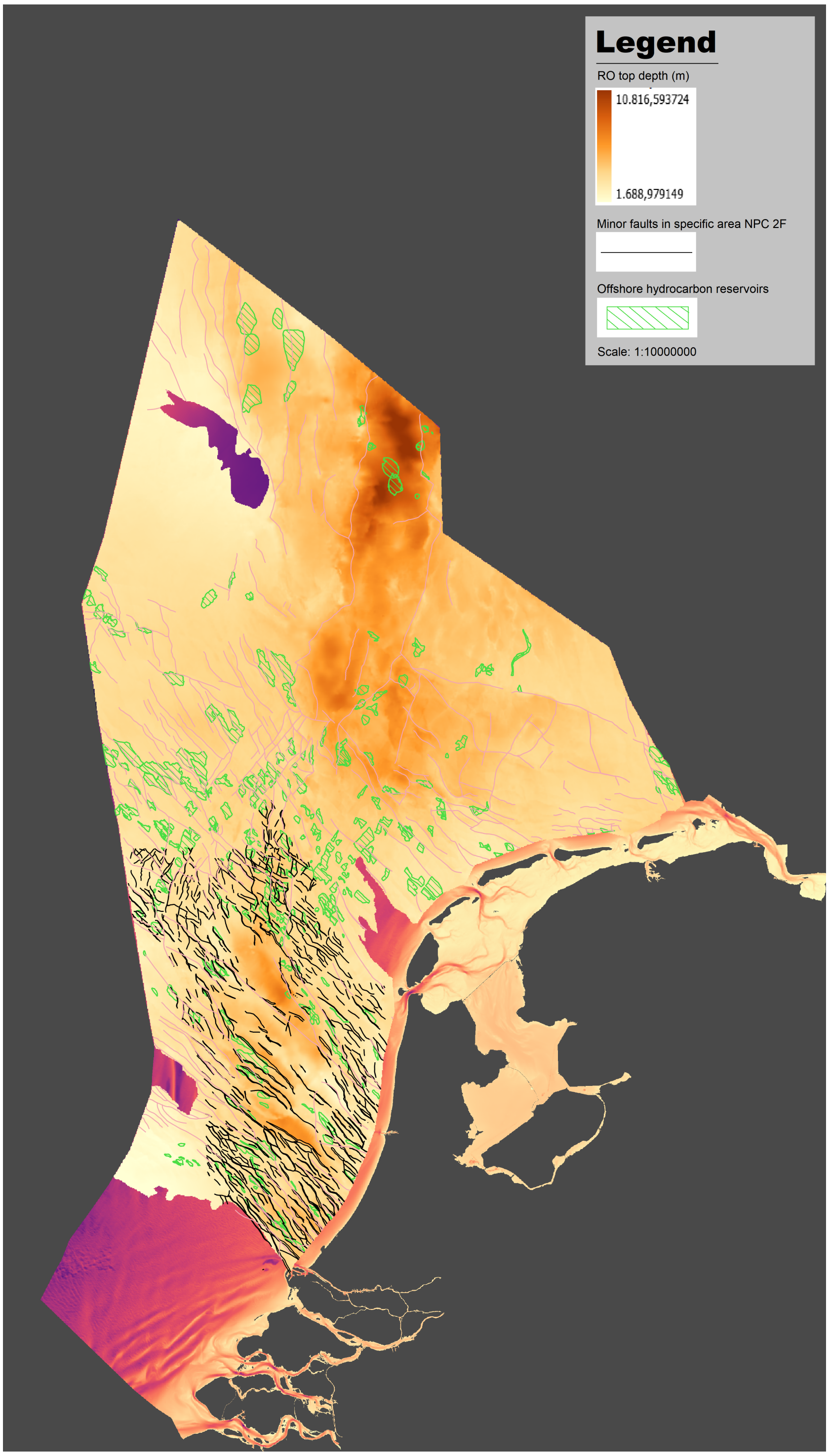

Figure B.5: QGIS model of the dutch offshore with interpolated RO top depths, minor faults and the hydrocarbon reservoirs present in the Dutch offshore

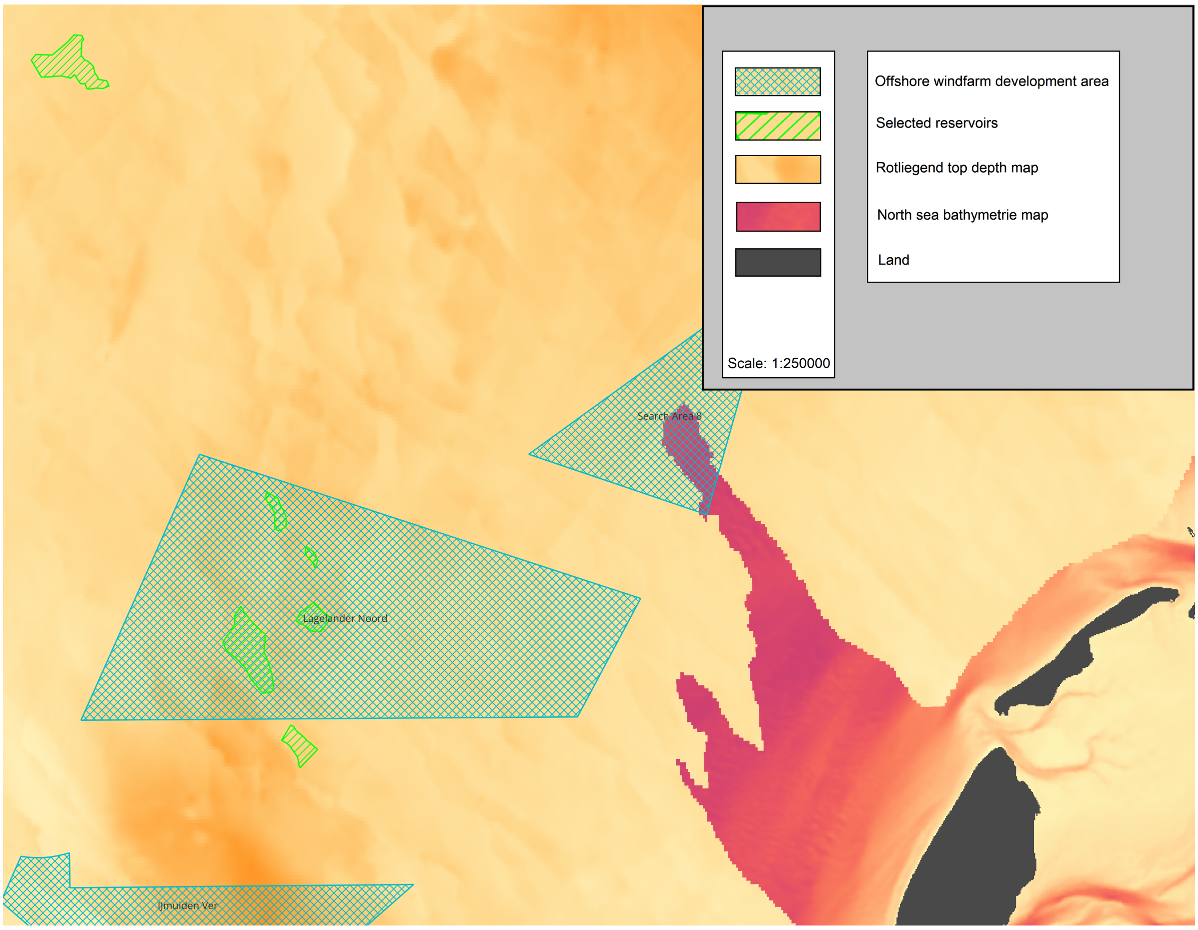

Figure B.6: QGIS model of the dutch offshore with the location of the offshore windfarm development areas and selected reservoirs